FINAL REPORT

ENVIRONMENTAL DURABILITY OF GRAPHITE/EPOXY COMPOSITES: THE COMBINED EFFECTS OF MOISTURE, CATHODIC POLARIZATION, AND STRESS

Christopher C. Pauly
Graduate Research Assistant

S. Ray Taylor, Ph.D.
Faculty Research Scientist

Jose P. Gomez, Ph.D.
Associate Director

Virginia Transportation Research Council
(A Cooperative Organization Sponsored Jointly by the
Virginia Department of Transportation and
the University of Virginia)

In Cooperation with the U.S. Department of Transportation
Federal Highway Administration

Charlottesville, Virginia

June 2002
VTRC 02-R13

DISCLAIMER

The contents of this report reflect the views of the authors, who are responsible for the facts and the accuracy of the data presented herein. The contents do not necessarily reflect the official views or policies of the Virginia Department of Transportation, the Commonwealth Transportation Board, or the Federal Highway Administration. This report does not constitute a standard, specification, or regulation.

Copyright 2002 by the Commonwealth of Virginia.

ABSTRACT

The increasing acceptance and incorporation of fiber-reinforced polymer matrix composites (PMCs) as engineering construction materials have led many to look to the infrastructure as an application for these versatile materials. One such system is pultruded graphite fiber-reinforced epoxy (graphite/epoxy). Some PMC systems degrade when subjected to environmental conditions (e.g., moisture, stress, UV light, electrochemical polarization). These variables are typically studied either singularly or in series, but in real applications (e.g., aerospace, marine, infrastructure), these materials are subjected to many of these conditions simultaneously.

To simulate field conditions, this study investigated the combined effects of an aqueous environment, electrochemical polarization, and applied bending stress on the durability of a pultruded graphite/epoxy composite. The findings indicate that graphite/epoxy composites cannot be assumed to be insensitive to degradation by environmental variables. Further, electrochemical polarization, as might occur with contact with a metal such as a fastener, can accelerate degradation. This damage requires the presence of moisture. Chloride and sulfate concentrations in rain are sufficient to establish an electrolyte within creviced regions, but deicing salts would overtake these as a contributor to conductivity.

Further findings may be summarized as follows:

- Application of polarization in an aerated 0.6M NaCl environment led to breakdown of the fiber/matrix interface. The high pH environment created during the oxygen reduction reaction was necessary but not sufficient to create this breakdown, as the unpolarized specimen exposed to a pH 13 environment did not degrade. Cathodic polarization as would occur by coupling to steel or aluminum is required.

- Application of cathodic polarization did not significantly alter strength. Average measurements of shear strength, however, did decrease with the application of cathodic polarization for 70 and 90 days.

ENVIRONMENTAL DURABILITY OF GRAPHITE/EPOXY COMPOSITES: THE COMBINED EFFECTS OF MOISTURE, CATHODIC POLARIZATION, AND STRESS

Christopher C. Pauly
Graduate Research Assistant

S. Ray Taylor, Ph.D.
Research Associate Professor

Jose P. Gomez, Ph.D.
Senior Research Scientist

INTRODUCTION

More than 25 percent of bridges in the United States have been rated as either structurally or functionally deficient,[1-5] which has led to significant expenditures for bridge maintenance. The average annual cost to maintain current highway and bridge conditions through the year 2013 is estimated to be $54.8 billion.[1] The current condition of the bridge inventory is due, in part, to the vulnerability of current construction materials (e.g., steel and concrete) to degradation by aggressive species commonly found in the environment (e.g., chloride, sulfate).

The vulnerability of steel to environmental degradation has led many transportation agencies to investigate advanced polymer matrix composites (PMCs) as alternative materials for infrastructure applications. The advantages of these PMCs include higher specific strength and stiffness properties, ease of fabrication, and resistance to corrosion. A graphite fiber-epoxy (graphite/epoxy) composite can have ultimate strength and stiffness similar to those of high performance steels while still being less than 20 percent of the weight. This system offers great promise in repair and retrofit of existing steel and concrete bridge superstructures. It is also being considered for use in pre-tensioning and post-tensioning cables for concrete construction. Though these materials do not "rust" in the conventional sense, the mechanical properties of composites can be degraded over time by various environmental factors including moisture, chemicals, light, and temperature.

More recently, PMCs filled with graphite fibers have been found to be affected by electrochemical polarization. This can occur when the composite is galvanically coupled to essentially any other metal (e.g., steel, aluminum) in the presence of moisture and ions.[2-4] Because of the electrochemical nobility of graphite, this coupling can lead to an increased corrosion rate of the metal and damage to the composite fiber/matrix interface as a result of the cathodic reaction (oxygen reduction) that is taking place on the graphite fibers. Although electrochemical polarization has been recognized as a damaging process in some polymer systems (e.g., polyimidies), it is not yet clear how the damage mechanisms translate to other resin chemistries (e.g., epoxy) being used in infrastructure applications. An additional obvious variable that effects the long-term mechanical performance of a composite is that of stress.

The effect of each of these variables (moisture, chemical environment, light, temperature, polarization, and stress) on the mechanical properties of PMCs has been traditionally studied individually, or at best, in series. However, in the field, composites will be exposed simultaneously to many, if not all, of these variable. To date, there have been essentially no studies on the combined effects of the conditions representative of the infrastructure on the mechanical durability of PMC composite materials.

PURPOSE AND SCOPE

The purpose of this study was to quantify the combined effects of moisture, cathodic polarization, and stress on the strength of a pultruded graphite fiber/epoxy matrix composite as a function of time. A secondary purpose was to determine if a nondestructive electrochemical measurement technique known as electrochemical impedance spectroscopy (EIS) could detect and monitor the degradation of this graphite/epoxy composite. The investigation incorporated EIS monitoring of all exposed specimens followed by a destructive test to quantify possible mechanical strength degradation. Scanning electron microscopy of fracture surfaces was also incorporated to determine the extent of damage and failure mechanisms for tested specimens.

METHODS

Materials

The material studied in this investigation was a pultruded unidirectional graphite/epoxy composite, consisting of 36K tow Hercules AS2 graphite fiber and Shell Epon 9310 epoxy resin The composite panels measured 152.4 cm long, 14 cm wide, and approximately 3.32 mm thick. The panel cross section contained 170 to 180 tows and had an average fiber volume fraction of 50.6 percent. Pultrusions were performed in one continuous run at Strongwell Inc. (previously Morrison Molded Fiber Glass) in Bristol, Virginia.

This material was the subject of an earlier mechanical characterization study.[5] This study determined that the fiber volume fraction ranged from 31 to 68 percent, indicating that the distribution of the fiber throughout the composite panel was uniform. Figure 1 shows a cross-sectional view of the material. Not all of the fibers are straight or parallel. Figure 2 shows the fiber orientations on the composite surface.

Preparation of Specimens

Test specimens were cut from the panels using a water-cooled diamond embedded high-speed wafer saw. Two types of specimen geometries were used: thick and thin. The thick specimen were 16.25 cm long; 1.27 cm wide; and 3.32 mm thick, the same thickness as the

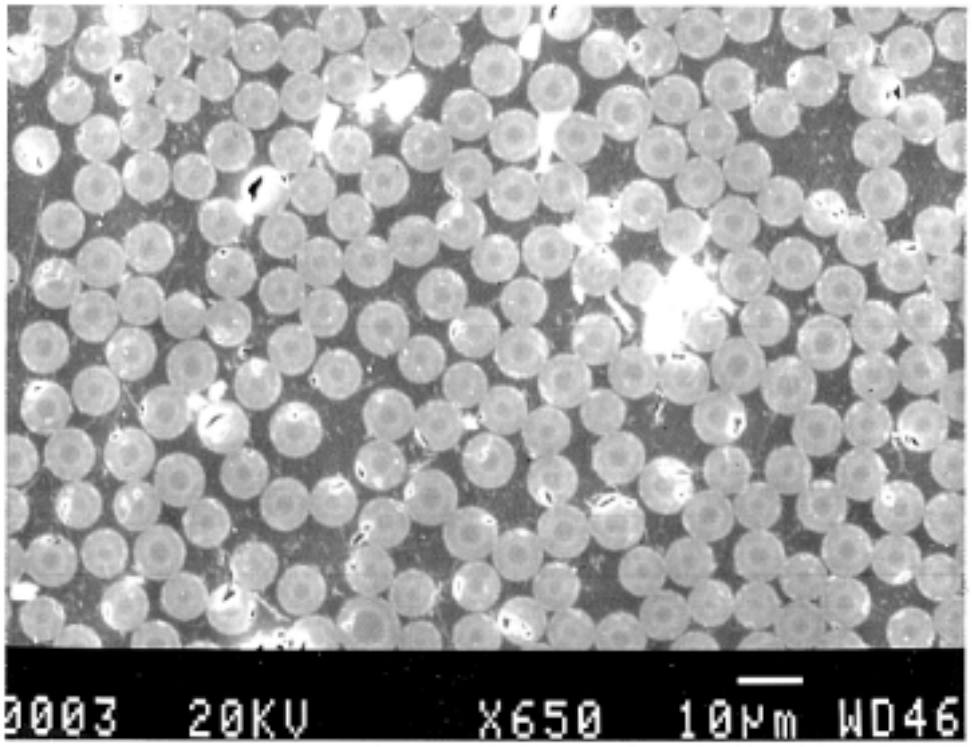

Figure 1. SEM micrograph of pultruded gr/epoxy composite cross section showing fiber distribution.

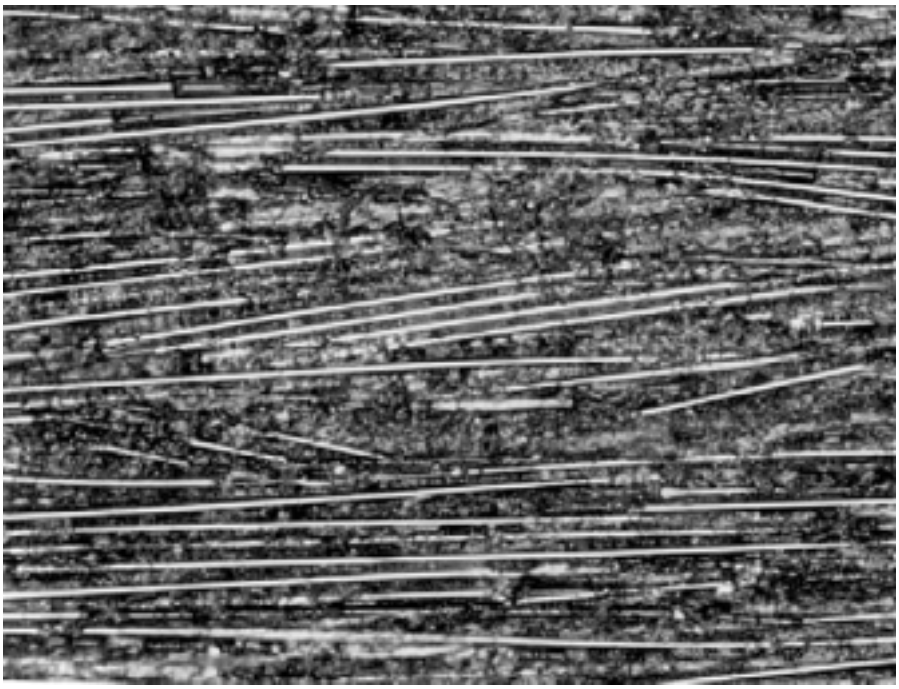

Figure 2. Optical micrograph of polished composite surface showing fiber misorientation (200x).

panel. The thin specimens consisted of a thick specimen cut in half and were 16.25 cm long, 1.27 cm wide, and from 0.71 to 0.86 mm thick.

Specimens were washed with an Alconox soap solution to remove any remaining residue from the oil/water mixture used as a blade coolant. The specimens were then abraded with 240 grit SiC (silicon carbide) paper under running distilled water to clean the surface further. This abrasion also removed the thin insulating layer of resin-rich material to expose clean fiber surfaces. After abrading, care was taken not to contaminate the composite surface with hand oils.

Specimen ends were coated with silver paint, which served as current collectors. Electrical connections were established using nickel ribbon embedded in the silver paint. This entire connection was then covered with epoxy for mechanical integrity. Figure 3 shows the specimen with electrical connections. Because of the anisotropic nature of graphite conduction, and the insulating properties of the epoxy, calculation of accurate resistivity values for the entire composite was difficult. Two-point resistance measurements in the end-to-end direction ranged from 10 to 20 Ω (ohms); in the end-to-face direction, measurements ranged from 20 to 40 Ω. Such a broad range of values is probably due to discontinuous or broken fibers within the composite and the varying path lengths for the current depending on the location of the measurement.

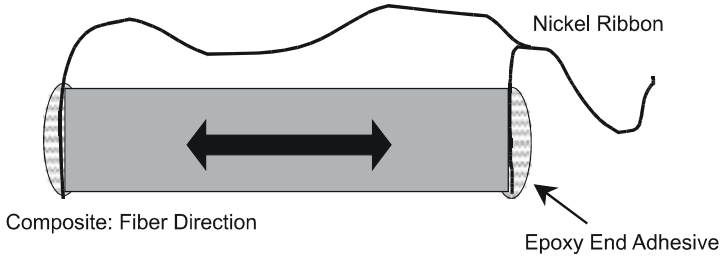

Figure 3. Electrical connections made to gr/epoxy composite.

Resistance measurements have been used to measure damage accumulation in composites.[6] The expression used to calculate resistance of a composite in the fiber direction is as follows:

$$R = (\rho_f L / b\ d\ V_f) + R_c$$

where ρ_f is fiber resistivity; V_f is volume fraction of unbroken fibers; L is length between electrodes; *b* and *d* are specimen width and thickness, respectively; and R_c is the contact resistance between sample and electrodes. Conduction through the thickness is highly dependent on fiber volume fraction and is similar in principle to percolation theory. In general, a V_f of 50 to 60 percent will ensure fiber contact and good electrical conduction; however, with an average V_f of 50.6 percent in this material, many regions will fall below this critical loading. Thus, because the fiber was not uniformly distributed throughout the composite material, such a range of resistance values is expected.

Figure 4 shows the directional terminology used throughout this study. The direction parallel with the fiber direction is *longitudinal*, the direction perpendicular to the composite face is *through thickness*, and the direction perpendicular to both the fiber orientation and through thickness is *transverse.*

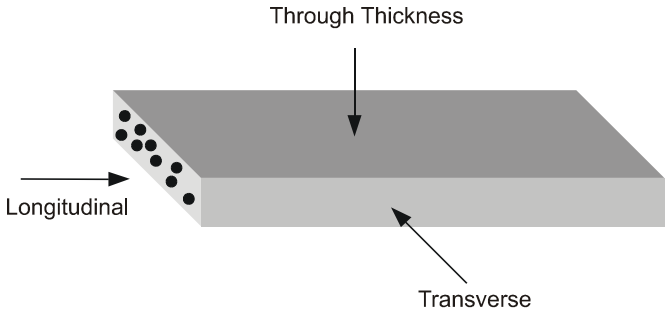

Figure 4. Gr/epoxy specimen showing directional terminology.

Electrochemical Testing

Baseline Data

Much of the baseline electrochemical characterization of the composite was performed using a standard electrochemical cell, shown in Figure 5. This cell exposed a 1-cm^2 area of the composite using a knife-edged Teflon gasket. A platinum-coated niobium mesh served as the counter electrode, and a saturated calomel reference electrode was used.

The baseline data provided information that was used to design subsequent experiments. To establish this baseline characterization of the composite, the following tests were run: open circuit potential (OCP) monitoring, cyclic voltammetry, polarization scans, and EIS.

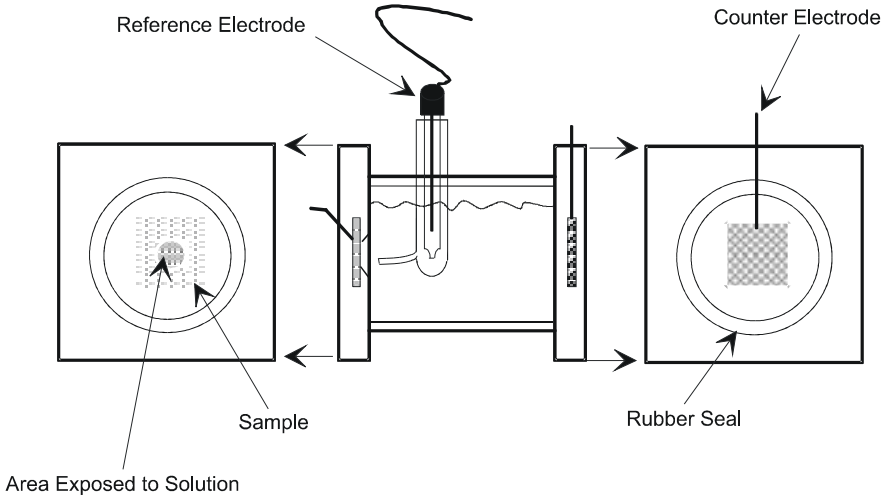

Figure 5. Electrochemical cell used to obtain baseline electrochemical data.

OCP. The OCP is the potential of a metal or conductive sample when immersed in an electrolyte. It is also known as the corrosion potential and is the potential at which the anodic and cathodic corrosion currents are equal. One goal in electrochemistry is to know the corrosion current or conduct interfacial characterization studies when a sample is in the freely corroding condition, i.e., at OCP.

Cyclic voltammetry. This is a means for characterizing the interfacial properties of an electrochemical interface by imposing an upward and downward voltage ramp and then measuring the current response. The data output plots the current against the voltage. This voltage ramp is swept through any number of cycles, hence the term *cyclic.*

Polarization scan. This electrochemical method is similar to cyclic voltammetry, except the voltage is swept at a very low rate and only one cycle of polarization is performed. The data are often plotted as voltage vs. log current since the current excursions in an electrochemical system can be quite large.

EIS. An AC-based electrochemical method whereby interfacial properties (e.g., charge transfer resistance, double layer capacitance, diffusional impedance) may be acquired at any potential. It is a method to determine corrosion characteristics at the OCP. It operates by imposing a low amplitude (10-20 mV) sine wave onto a DC bias potential (e.g., OCP) and comparing the voltage current characteristics. Impedance is simply a vector (has a magnitude and direction) composed of the ratio of the voltage signal compared to the current signal. The direction of the vector is determined by the phase difference between the voltage and current. If the preceding operation is performed over a range of excitation frequencies, an impedance spectra of an electrochemical interface is acquired.

Electrochemical tests were conducted at room temperature using aerated 0.6 M NaCl as an electrolyte. Specimens were prepared using the procedure previously described.

Combined Exposures

To test the composite samples under combined conditions of an aqueous environment, electrochemical polarization, and stress, a novel cell design was developed. A schematic of the cell is shown in Figure 6. The cell consisted of a Plexiglas trough with slots machined through the sides so that specimens could be inserted. After the sample coupons were inserted and the slots were sealed with a silicone sealant, a three-point loading jig was affixed to each specimen. The load was applied by a central screw having a machined fiberglass rod at the end to provide a line load in the transverse direction. The number of screw turns needed to achieve a specific strain was determined by the use of a strain gage affixed to a test specimen. The applied strain used in stressed samples was 0.5 percent in the outer fibers, applied via a three-point bend. This was one-half the ultimate tensile strain as determined by previous research.[5]

The cell used a typical three-electrode configuration for electrochemical polarization and EIS monitoring. The composite specimen served as the working electrode, a platinum-coated niobium mesh counter electrode was positioned under each specimen, and a saturated calomel

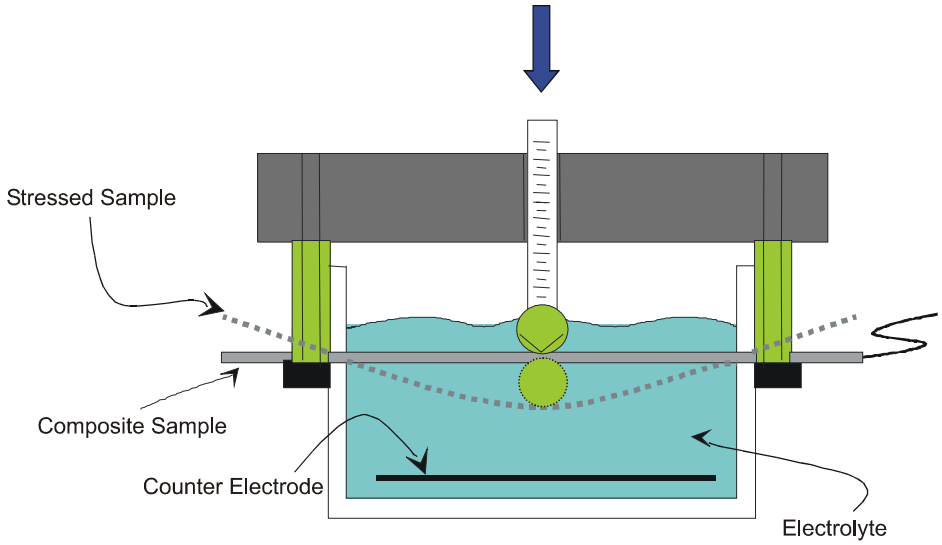

Figure 6. Electrochemical cell used to expose gr/epoxy composite samples to immersion, polarization, and bending stress.

electrode (SCE) was used as the reference electrode for all experiments. Each cell could accommodate 10 specimens for exposure and testing. This configuration allowed for prolonged polarizations with in situ OCP monitoring and EIS testing of individual specimens.

Thick Specimens

The thick specimens described previously were used for the first set of exposures. Four exposure conditions were investigated. Seven specimens were exposed to each of the four exposure conditions:

1. control (open to air)

2. immersion (aerated 0.6 M NaCl)

3. immersion (aerated 0.6 M NaCl) + polarization (-1.2 V_{SCE})

4. immersion (aerated 0.6 M NaCl) + polarization (-1.2 V_{SCE}) + stress (0.5% strain).

An exposure of immersion + stress was also planned, however, limitations involving material supply precluded this exposure condition from being in the test matrix. Exposures lasted for 30 days. During the exposure time, EIS scans were taken periodically. The EIS scans used a 10 mV rms amplitude excitation centered about a DC potential of 0 V_{SCE} (0 volts versus an SCE). The frequency scan range was 50 kHz to 50 mHz. EIS measurements were taken using a PAR 273A potentiostat with a Schlumberger 1255 Frequency Response Analyzer. At the end of 30 days of exposure, samples were removed from the tanks for mechanical testing.

Thin Specimens

Thin specimen testing was designed to clarify issues that became apparent after testing of the thick specimens. The reasoning for this change in specimen geometry is discussed in detail later. Exposure conditions for the thin specimens were identical with those for the thick specimens. Eight specimens were exposed to each condition for 70 days. An additional set of exposures was exposed for 90 days using the following exposure conditions:

1. immersion (aerated 0.6 M NaCl) + polarization (-1.2 V_{SCE})

2. immersion (aerated 0.6 M NaCl) + polarization (-1.2 V_{SCE}) + stress (0.5% strain).

EIS measurements were made periodically throughout the exposures. The scanned frequencies remained the same, but the maintained DC potential was changed from 0 V_{SCE} to 0 V_{OCP} (0 volts vs. OCP). This change was made because the spectra were changing slowly as each specimen was tested in series. This change was independent of the specimen testing order. The OCP of the composites climbed to approximately +0.5 V_{SCE} over 1 hour after being released from polarization at -1.2 V_{SCE}. Therefore, by testing at 0 V_{SCE}, the specimens were being tested at a slight cathodic overpotential. This overpotential increased with each specimen as the OCP climbed with time. For this reason, specimens were allowed to establish a stable open-circuit potential before testing. Testing was carried out at 0 V_{OCP} to avoid cathodic polarization during scans. This change did not invalidate the thick specimen tests at 0 V_{SCE} because comparisons and changes were noted over time for each specimen, not between specimens.

Mechanical Testing

To examine the effects of exposure conditions on composite durability, mechanical testing of the samples was necessary. Two types of tests were used to measure strength, as described in the following sections.

Mechanical testing was performed using an Applied Testing Systems (ATS) screw driven mechanical testing frame, with a 22.24 kN load cell. Load and displacement data were taken using a computerized data acquisition system called Chartrec.

Three-Point Bend Test (Thick Specimens)

The bending test was used to measure the flexural strength of the thick specimens after exposure. The tests were carried out using an MTS three- or four-point bend test fixture (Model 642.10B). A picture of the test setup is shown in Figure 7. Span length was 12.7 cm, which yielded a span/depth ratio of approximately 38. The tests were quasi-static with a cross-head displacement rate of 2.54 mm/min.

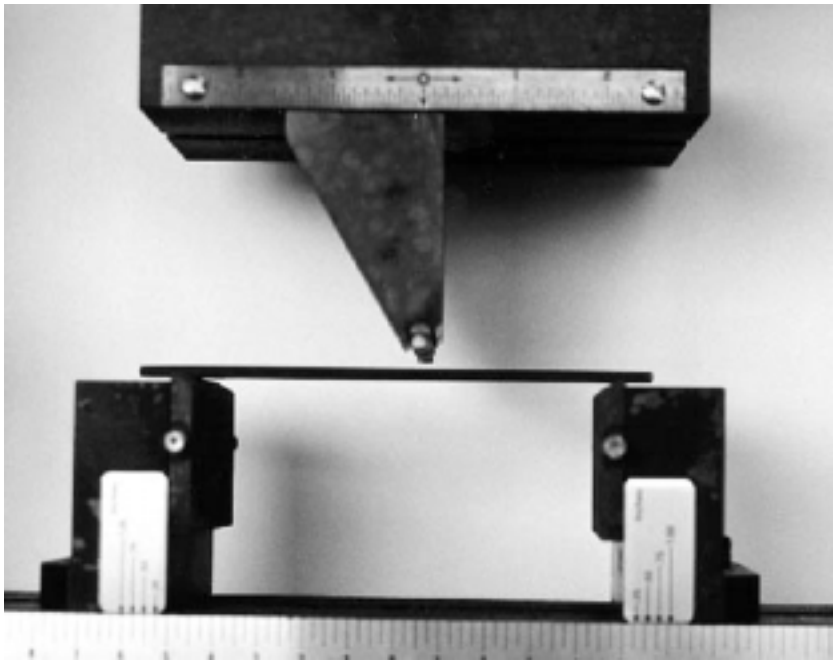

Figure 7. Three-point bend test rig with composite specimen.

Davis Test (Thin Specimens)

The Davis test has been used to characterize strength degradation in bismaleimide (BMI) composites.[7] This test incorporates angled notches in the sides of the sample coupon and uses tensile loading to avoid a buckling failure.

A photograph of the test configuration and specimen dimensions is shown in Figure 8. Specimens were tested soon after removal from the exposure tanks and were kept submerged in distilled water after removal from the tank to prevent drying before the test. The specimen notches were hand cut using a jeweler's blade while specimens were held in a pre-notched jig that allowed for consistent cutting of specimens. The notches were cut at an incline of 45 degrees, and the distance between notch tips was 3.8 cm. This allowed for a notch length/specimen width (L/b) ratio of 3. The quasi-static tests were run with a cross-head displacement of 0.254 mm/min.

The presence of notches in the sample will cause a stress concentration at the tips of the notches. However, this study investigated the changes in strength caused by the application of environmental exposures. If all specimens (control and exposed) are of the same geometry, valid comparisons can be made to quantify changes in mechanical properties.

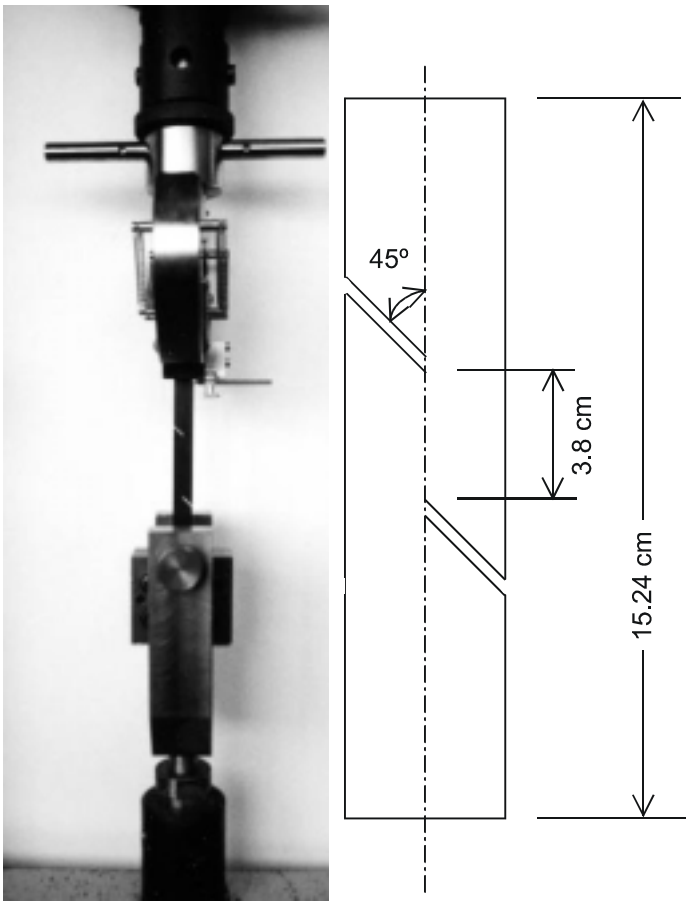

Figure 8. Testing grips for the Davis test and detail of Davis test specimen.

RESULTS AND DISCUSSION

Thick Specimens

Baseline Electrochemical Data

Potentiodynamic Tests

Figure 9 shows polarization curves for the graphite/epoxy composite in aerated 0.6 M NaCl. The cathodic scan was initiated 10 mV anodic to the OCP, and the applied potential was scanned in a negative direction at 1 mV/sec. In this scan, the OCP was +220 mV_{SCE}. Because of the highly polarizable nature of the material, initial open circuit values ranged from -50 to +300 mV_{SCE}. After being released from a cathodic potentiostatic hold, the open circuit often rose to values as high as +550 mV_{SCE}. This change is most likely attributable to changes in the surface chemistry of the graphite fibers. The functional groups present at the graphite-electrolyte interface play very important roles in determining the electrochemical behavior of carbon and

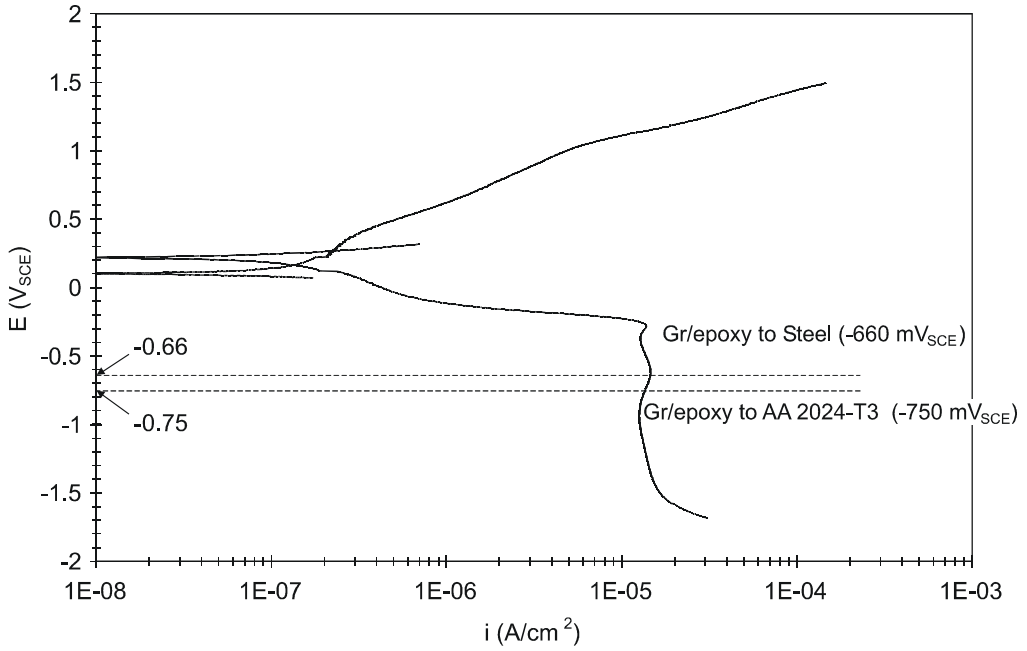

Figure 9. Anodic and cathodic polarization scans of gr/epoxy composite in 0.6 M NaCl (ambient aeration), scan rate = 1 mV/sec. Also shown are potential values for galvanic couples of gr/epoxy to steel and gr/epoxy to aluminum.

graphite.[8,9] Changes in the structure or type of functional group can greatly affect the electrocatalytic behavior of the electrode.

Some of the functional groups suggested to be present on carbon and graphite surfaces include carboxylic groups, phenolic hydroxyl groups, and quinone-type carbonyl groups.[10] The actual structure or types of functional groups present on the surface of this composite were not studied in this investigation. However, the presence of these groups must be acknowledged as they are important species that affect the electrochemical nature of this composite material. In this case, cathodic polarization may be altering the structure of certain functional groups present on the graphite fiber surface, either through direct electron transfer or through a change in the local electrolyte chemistry brought on by the reduction of oxygen. Any change to the functional groups could account for the noticeable increase in OCP resulting from an extended cathodic polarization.

As can be seen in Figure 9, from open circuit to -300 mV_{SCE} there appears to be two regions of different slope. These may be due to differences in O_2 reduction kinetics between basal and edge orientations of the exposed graphite fibers.[8,9] At potentials negative of -300 mV_{SCE}, the current enters a potential independent region. In the potential window from -300 to -1700 mV_{SCE}, the cathodic current is limited by the diffusion of oxygen through the solution to the composite surface. The limiting current density is approximately 15 $\mu A/cm^2$. As the potential is lowered below -1.5 V_{SCE}, the current again increases because of hydrogen evolution.

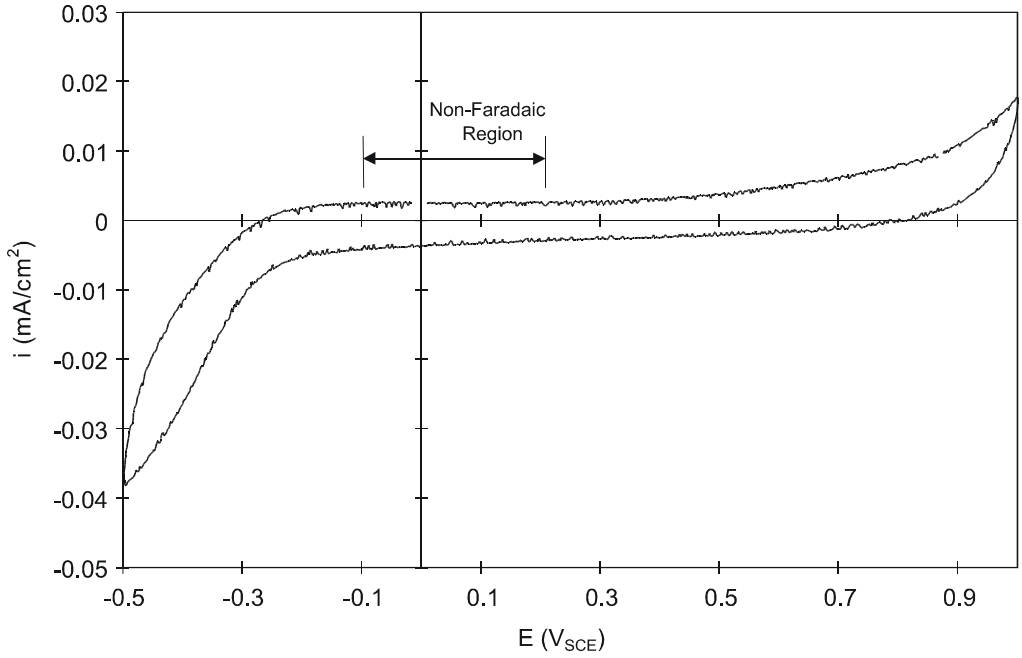

Figure 10. Cyclic voltammagram of gr/epoxy in areated 0.6 M NaCl with non-Faradaic region shown. Scan rate = 20 mV/sec.

Figure 9 also shows potential values for galvanic couples between graphite/epoxy composites and carbon steel and between graphite/epoxy composites and aluminum (AA 2024-T3). Galvanic couples were created by bolting a 6.5 cm^2 composite sample to a metal specimen of similar dimensions with a plastic bolt. The specimens were then immersed in a 0.6 M NaCl solution and OCP measurements were made. Both of these galvanic couples induced a cathodic overpotential on the graphite/epoxy composite that is within the diffusion limited region of the oxygen reduction reaction.

The anodic polarization scan, also shown in Figure 9, was initiated 10 mV cathodic to the OCP. The potential was then scanned in a positive direction at 1 mV/sec. Two general Tafel regions are apparent as the anodic overpotential is increased. The first region is between the potentials of 0.5 and approximately 1.1 V_{SCE} and has a slope of approximately 500 mV/decade. The reversible potential for the oxygen evolution reaction is 0.53 V_{SCE} at a pH of 7.7, and is thus assumed to be the predominant anodic reaction within these potentials. At potentials greater than 1.1 V_{SCE}, the Tafel slope decreases to 250 mV/decade. Given the reversible potential of 1.1 V_{SCE} for chlorine evolution in a 0.6 M NaCl solution, this reaction adds to the anodic current at potential values above 1.1 V_{SCE}, accounting for the decrease in Tafel slope. Other investigators had identified these reactions as the predominate reactions on carbon in 0.6 M NaCl solution.[11]

To investigate the possibility of other surface reactions taking place, such as adsorption or oxide formation, cyclic voltammetry was incorporated. By investigating the current-potential behavior on a linear scale, information pertaining to surface reactions can be obtained that are

difficult to detect using the log scale of a polarization scan. Figure 10 shows a cyclic voltammagram (CV) for the composite material in aerated 0.6 M NaCl at a scan rate of 20 mV/sec. At high anodic overpotentials (>1000 mV_{SCE}) the current increases rapidly with potential as oxygen is evolved from the composite surface. At cathodic overpotentials greater than -300 mV_{SCE}, the current again increases with overpotential as dissolved oxygen is reduced to hydroxyl ions. The absence of peaks between these potentials suggests that the surface is highly polarizable with no charge transfer reactions taking place within the open circuit range. The fact that graphite is a highly polarizable material indicates that its potential can be moved around easily without eliciting an electrochemical reaction. Graphite is a very noble material. It is actually more noble than platinum. Thus, any contact to an engineering alloy such as steel will form a significant galvanic cell. It will cause accelerated corrosion of the metal and degradation of the composite.

Within this open circuit range, all current goes into charging or discharging the double layer capacitance. This capacitance can be calculated from the following equation:

$$i = C\frac{dV}{dt}$$

where i is the current, C is capacitance, and dV/dt is the scan rate. The potential window where this charging takes place is known as the non-Faradaic region, as Faradaic reactions involve transfer of charge. CV measurements were taken at scan rates of 5, 20, 40, and 80 mV/sec. All scans showed smooth non-Faradaic regions within the same potential windows and revealed current peaks at high cathodic and anodic overpotentials. Capacitance measurements from these tests are given in Table 1. Scan rates of 20, 40, and 80 mV/sec yielded similar capacitance values. The measurement taken at 5 mV/sec, however, yielded a higher value. This could be due to a higher amount of exposed fibers for the particular sample. The surface area of the exposed fibers is difficult to calculate or measure; therefore, capacitance values are given in terms of exposed composite area. The actual fiber surface area of each specimen will vary from coupon to coupon.

Table 1. Double Layer Capacitance Measurements of Composite Calculated From Cyclic Voltammograms at Varying Scan Rates

Scan Rate (mV/s)	Capacitance ($\mu F/cm^2$)
5	203
20	119
40	117
80	106

Polarization Studies

Although polarization experiments indicate that the graphite in composite electrodes may have different levels of electrochemical efficiency, they are generally non-reactive at and around

the OCP as evidenced by cyclic voltammetry. Of importance is the fact that galvanic coupling of these composites to conventional engineering alloys such as steel and aluminum polarizes the composite to potentials in which oxygen reduction is the dominant reaction. Oxygen is a ubiquitous cathodic fuel in atmospheric exposure. The reduction of oxygen produces hydroxyl species as a final product, but it also produces peroxide and superoxide radical intermediates. Hydroxyl ions are very wetting and can break down adhering interfaces such as a coating and metal or a graphite fiber and polymer matrix. Thus, the final product of oxygen reduction can start degrading the very essence of a composite, which is the adhesion of the fiber to the matrix. In addition, the peroxide and radical intermediates produced as intermediates in the reduction of oxygen can be damaging to the polymer matrix.

EIS

Figure 11 shows the Nyquist and Bode plots for data collected from an unpolarized composite sample exposed to aerated 0.6 M NaCl for 6 days. No detectable changes occurred on the surface of the composite over this period. The impedance response is very capacitive in nature as can be seen by the phase angle values of almost -90 degrees at low frequencies and the steep slope of the Nyquist plot. At high frequencies (>1000 Hz), the capacitive response is short circuited and the measured impedance becomes equal to the solution resistance. This is seen in both Bode plots as the phase angle approaches 0 and the magnitude levels off at a value equal to the solution resistance. At very high frequency, the phase angle tail becomes slightly positive. This is probably due to inductance of the lead wires. Measurements at very high frequencies (>10 kHz) were not used for analysis because of limitations imposed by the reference electrode.

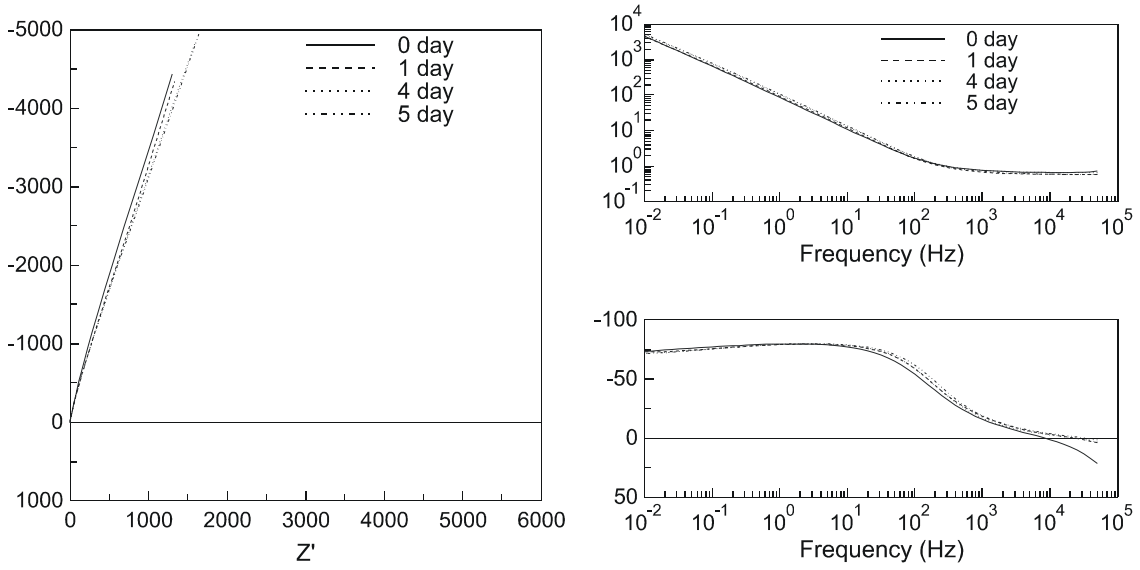

Figure 11. Nyquist and Bode plots for EIS data of unpolarized gr/epoxy composites. No change in impedance data is apparent for 5-day exposure.

Figure 12 shows the Nyquist and Bode plots for data collected from a composite sample that was polarized to -1.2 V_{SCE} for 24 hours. Scans were taken at 0, 1, 6, 12, and 24 hours. A very noticeable change is apparent in both the Nyquist and Bode phase angle plots. This change consisted of a decrease in impedance as polarization time increased. This is best seen in the Bode phase angle plot as a drop in phase angle at the lower frequencies. This change occurs over a 24-hour period.

This decrease in phase angle at low frequencies can also be interpreted as a decrease in polarization resistance (R_p). The value of R_p can be represented as the diameter of a semicircle fit to the Nyquist plot. From an analysis of Figure 12, a semicircle fit yields a progressively smaller diameter with time. R_p is inversely proportional to the rate of the charge transfer reaction taking place on the electrode surface. A change in R_p can be brought about by many physical changes. Some of these are a change in electrode surface area, a change in the local chemistry of the electrode/solution interface, and a change in the catalytic efficiency of the electrode.

Although diffusion is not apparent from the electrochemical impedance spectra, it cannot be ruled out. Thus, the term R_p was chosen instead of R_{ct} (charge transfer) to describe all of the processes occurring in parallel with the interfacial capacitance.

Electrode surface area changes can be discounted as a reason for the change in R_p. This can be deduced by measuring the capacitance of the electrode surface. Capacitance is measured in units of Farads/area. Therefore, assuming a relatively stable intrinsic electrode capacitance, a change in electrode surface area will result in a change in the measured capacitance. One way to measure capacitance is by using the Bode magnitude plot. This can be rearranged to solve for capacitance by:

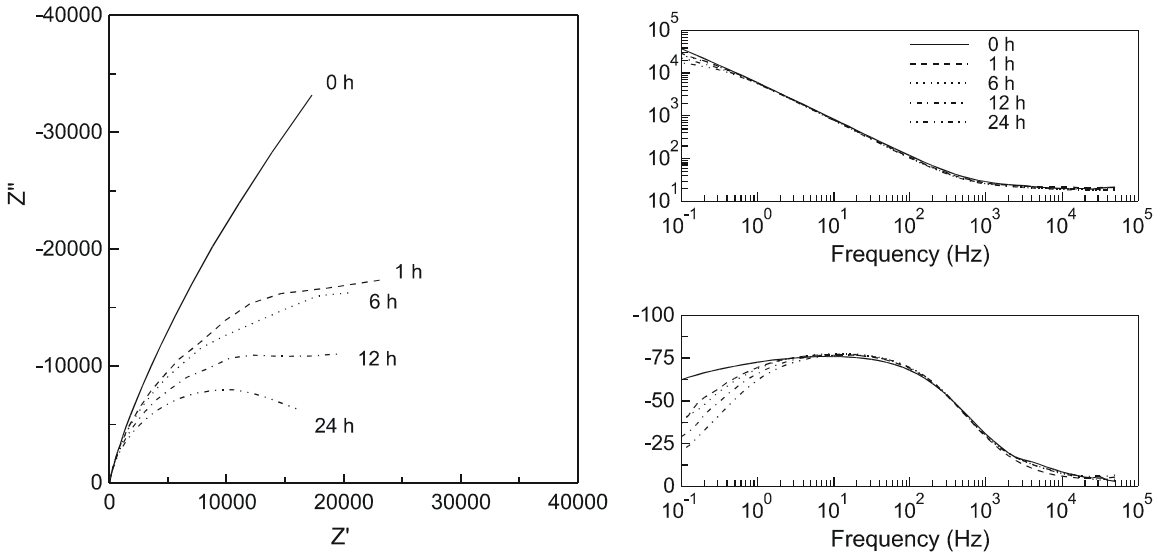

Figure 12. Nyquist and Bode plots for gr/epoxy composite polarized at -1.2 V_{SCE}. Impedance data yield decreasing R_p over 24 hours.

$$Z_c = 1 / (j\ \omega\ C) \quad \Rightarrow \quad C = 1 / (j\ \omega\ Z_c)$$

where Z_c is the impedance of a capacitor, $j = (-1)^{1/2}$, and C = capacitance. By fitting a line to the sloped region in the Bode magnitude plot and determining the value of Z where $\omega = 1.0$, the capacitance can be calculated as simply:

$$C = 1 / (Z * 1.0)$$

From the Bode magnitude plot in Figure 12, it is evident that the sloped portion of the curve does not change until the frequency is less than 1 Hz. The measured capacitance and thus electrode surface area, therefore, remained constant throughout the 24-hour exposure.

Changes in the local solution chemistry are expected to occur with the application of polarization. Before the impedance spectra was measured, however, the specimen was released for several hours from polarization and was allowed to re-establish a stable OCP. In that time, equilibration of local chemistry differences should have occurred through standard convection. This did not occur, so that differences in local solution chemistry at the boldly exposed graphite surface do not contribute to the observed changes in impedance data. However, it is possible that local chemistry changes were taking place in a creviced geometry and thus were not subjected to bulk convection of the solution. To investigate this, a specimen was polarized to -1.2 V_{SCE} for 5 days. The cell was then emptied and circulated with dry air for 1 week so the specimen surface was able to dry fully. The cell was then re-filled with solution, and EIS measurements were taken. The specimen was not polarized after the cell was re-filled with solution. Figure 13 shows the Bode plot for this test. The scans performed after the specimen was allowed to dry are identical with those taken immediately after cathodic polarization. These tests suggest that a cathodic polarization induces a permanent change in the morphology. This change could be surface roughening, or alteration of the composite surface chemistry, but it is not a change in the local solution chemistry.

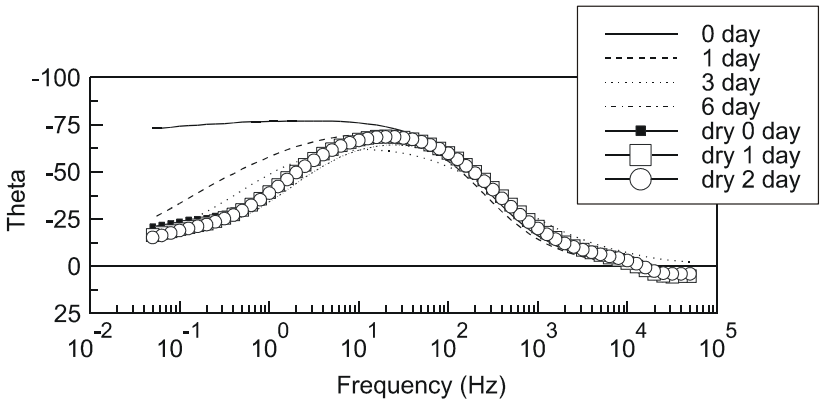

Figure 13. Bode phase angle plot showing EIS data for gr/epoxy polarized at -1.2 V_{SCE}, for 6 days; specimen was allowed to dry, and cell was re-filled and scanned at 0-, 1-, and 2-day intervals.

It is possible that the catalytic efficiency of the electrode could be changing with application of cathodic polarization. The products from the reduction of oxygen may change or destroy fiber sizing that is applied to enhance fiber/matrix bond strength. The reduction of oxygen to hydroxyl ions creates a localized environment of elevated pH. If the fiber sizing is unstable in an alkaline environment, it could very well be dissolved in a matter of hours.

As discussed earlier, the cathodic reduction of oxygen may also affect the chemistry of functional groups attached to the graphite fibers. Oxygen is a ubiquitous cathodic fuel in atmospheric exposure. The reduction of oxygen produces hydroxyl species as a final product, but it also produces peroxide and superoxide radical intermediates. Hydroxyl ions are very wetting and can break down adhering interfaces such as a coating and metal or a graphite fiber and polymer matrix. In addition, the peroxide and radical intermediates produced as intermediates in the reduction of oxygen can be damaging to the polymer matrix. These functional groups greatly affect the electrochemical nature of graphite.[8,9] If the end-groups present on the fibers of this composite are being permanently altered by either the products of oxygen reduction or by direct reduction, it is very possible that these changes could be evidenced by changes in impedance measurements.

Figure 14 shows the effect of polarization level on the rate of phase angle depression. Samples were held at varying levels of polarization (0, -0.2, -0.4, -0.6, -1.2 V_{SCE}). To track the drop in R_p, the phase angle at a frequency of 0.1 Hz was plotted as a function of time. From this figure, it is evident that the drop in phase angle and the rate at which it drops are highly dependent on the level of applied polarization. It should be stated again that these potentials correspond to the value of cathodic polarization applied to the sample only during exposure. All EIS scans were performed at the OCP.

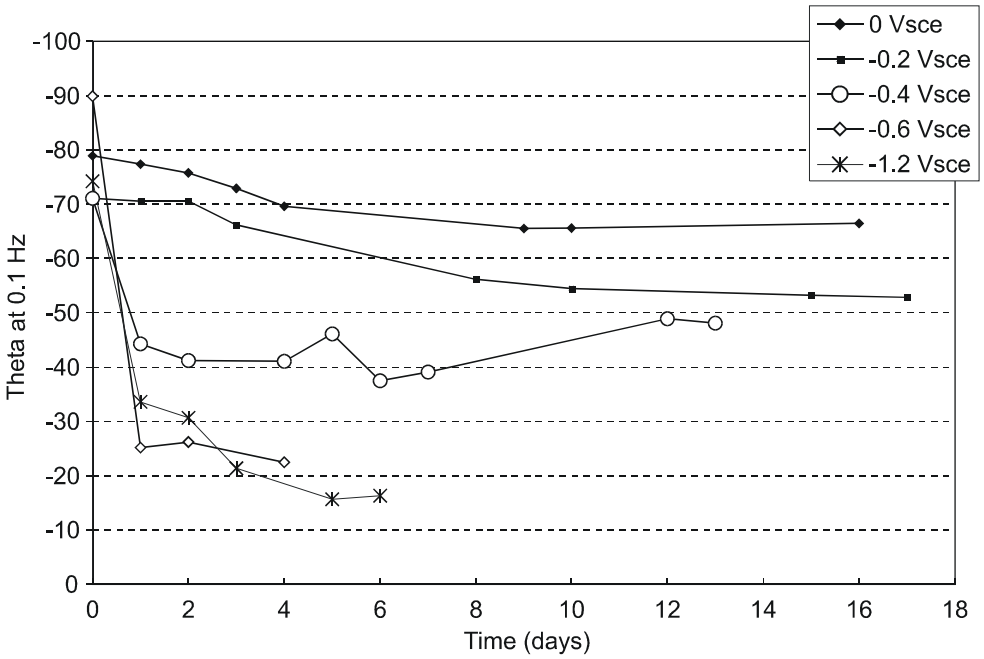

Figure 14. Bode phase angle at a frequency of 0.1 Hz showing effect of increasing cathodic overpotential on drop in low-frequency phase angle.

Combined Electrochemical and Mechanical Stress

Immersion

A total of 7 specimens were immersed in aerated 0.6 M NaCl. Figure 15 shows typical data taken over a 30-day exposure period. These specimens were under no applied polarization. From investigation of the EIS data, it appears that no detectable change in the composite surface occurred during this exposure time. This result is in agreement with the results for EIS spectra of unpolarized samples.

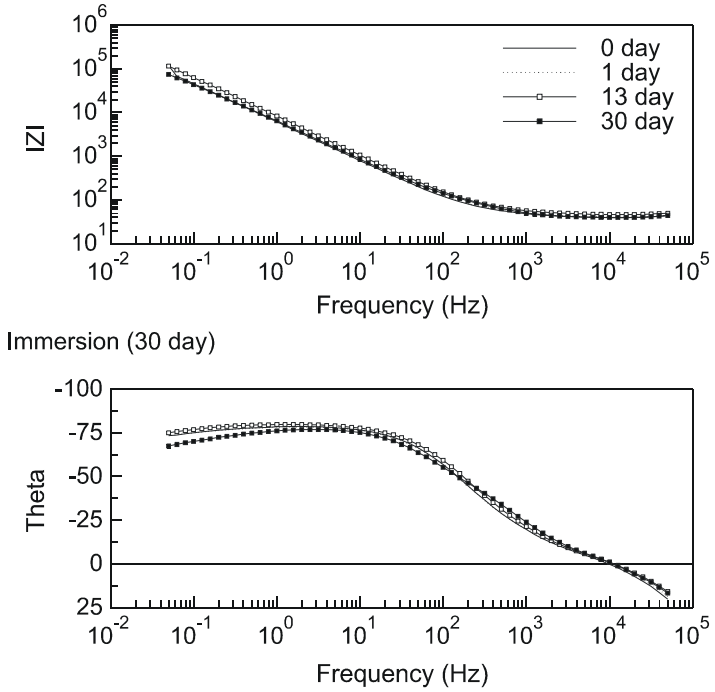

Figure 15. EIS data for unpolarized gr/epoxy composite (Tank A, No. 7) showing no apparent change over 30-day exposure period.

Immersion + Cathodic Polarization

Figure 16 shows typical EIS data for a specimen polarized to -1.2 V_{SCE} for 30 days. It is apparent that polarization has an effect on the impedance spectra of this graphite fiber/epoxy matrix composite. Four major changes were apparent from the impedance data. These changes are most easily seen in the Bode phase angle and magnitude plots.

Before these changes are explained, it should also be noted that the Bode magnitude plot shows varying values for the high-frequency plateaus. The impedance magnitude at high frequency is equal to the solution resistance, R_s. All impedance data showed variability in the measured values of R_s. These changes could be due to changes in surface area, but there is no apparent trend for the R_s values over time, nor do other area sensitive measurements, such as capacitance, show the same variability. It is suspected that these changes are due to differences

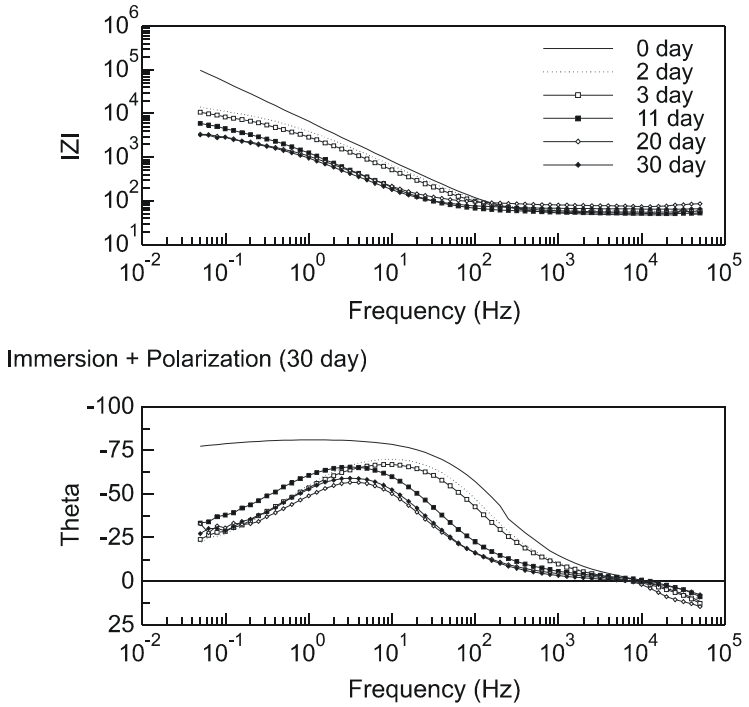

Figure 16. EIS data for a 30-day exposure of gr/epoxy to polarization of -1.2 V_{SCE} (Tank B, No. 4). Impedance magnitude data show an increase in capacitance. Phase angle data show drop in R_p after first day; phase angle peak decreases and curve shifts to left with time.

in the contact resistance of the alligator clips used to make electrical connection with the composite specimens. These clips were exposed to essentially a moist salt-fog environment because of the aeration of the 0.6 M NaCl solution. These copper clips visibly corroded during the entire test period, suggesting that the contact resistance was also changing during the exposure time.

The first major change in the impedance data was the drop in phase angle at low frequency after polarization for 1 day. This decrease in phase angle occurs within the first 24 hours of exposure and appears to reach a minimum after this time. The phase angle remains depressed at the low frequencies for the remainder of the test. This drop in R_p is probably attributable to changes in either fiber sizing or the chemical functional groups on the fiber surface. These are the same changes discussed previously.

Three other changes in the impedance spectra occur more slowly and become apparent over the 30-day exposure: (1) a decrease in phase angle values within the frequency range of 1 to 1000 Hz, (2) a gradual shift to the left (low frequencies) of the phase angle curve, and (3) a decrease in the slope and magnitude of the impedance with time.

After the initial low-frequency drop in phase angle during the first 24 hours of polarization, phase angle values within the frequency range of 1 to 1000 Hz continue to decrease. This is best shown by changes in the phase angle peak; however, phase angle values over the

entire 1 to 1000 Hz decrease. The phase angle peak shifts towards lower frequencies with extended polarization times, but this is due to a different mechanism and is discussed later.

The drop in phase angle resembles the "squaring effect" seen with the development of porous electrode behavior.[12,13] de Levie developed expressions describing the impedance of a porous electrode. This squaring effect amounts to a halving of the phase angle value as the electrode surface changes from planar to porous. In addition, as a porous response is developed, the impedance magnitude also decreases, approaching the square root of the original planar response. The Bode phase angle plot in Figure 16 shows this change from a planar electrode response to that of a porous electrode in the frequency range from 1 to 1000 Hz with increasing duration of cathodic polarization. The phase angle does not attain exactly ½ of its original value, but the equations developed by deLevie were for an idealized electrode. It cannot be assumed that the initial composite response was ideally planar or that the "pores" developed on the composite were a well-defined and consistent geometry, as assumed in de Levie's derivations.[14]

The other change in the Bode phase angle plot is the apparent shift to the left of the curve, especially noticeable in the frequency range of 1 to 1000 Hz. This shifting of the curve indicates an increase in the time constant, τ, for the system, where τ is the product of a capacitor and resistor in parallel:

$$\tau = R\,C$$

As can be seen in the equation, the value of τ can be altered through changes in the capacitance, C, or the resistance, R. It is possible for almost every imaginable fiber/matrix/ solution geometry to be present on a composite surface. This wide diversity of physical presentations gives rise to a distributed value for τ as the response of all the individual τs are averaged during the EIS measurement. Figure 17 shows a few typical physical representations of how a time constant can be realized on the composite surface.

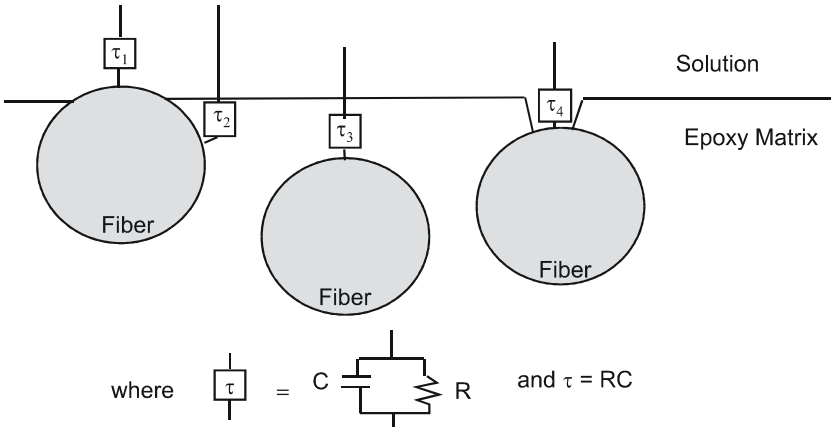

Figure 17. Various physical interpretations of time constant that could be expected for gr/epoxy composite. τ_1 - fiber exposed directly to solution, τ_2 - thin layer of matrix material covering fiber, τ_3 - fiber completely below epoxy surface, τ_4 - fiber exposed to solution through pore or cracked matrix material.

Area changes alone would not normally be expected to change τ because capacitance is inversely proportional to area (Farads/area) whereas resistance is proportional to area (Ohms x area), so that area effects cancel when τ is calculated. This assumption of area insensitivity for the time constant, however, assumes that all surface area is equally reactive. As porosity develops in this material, previously unexposed fiber surface comes in contact with the solution. This freshly exposed fiber surface may be less reactive because of fiber sizing that was not removed during initial composite abrasion. If this is the case, resistance changes attributable to increased surface area will not be proportional to the area change. As the area increases, however, the capacitance will increase proportionally. If the decrease in resistance is not proportional to the area change but the capacitance increase is, a shift in the time constant will result.

Another explanation for the shift in τ can be understood if fibers that are just below the electrode surface, or ones that are covered by a thin layer of matrix, are considered. In this case, the overlying polymer can be thought of as a coating. The expression for coating capacitance is

$$C_{coating} = \frac{\varepsilon_o \kappa d}{A}$$

where $C_{coating}$ is the coating capacitance, ε_o is the permittivity of free space, κ is the dielectric constant of the coating, d is the coating thickness, and A is the surface area of the electrode (i.e., fiber). Changes in this coating capacitance can therefore be influenced by area changes, changes in coating thickness, and changes in the dielectric constant.

The effects of area have previously been discussed for the case of double-layer capacitance measurements. Coating thickness, d, is not expected to contribute to changes in the capacitance measurement because of the random distribution of fiber depth and thus the "coating" thickness present over the entire electrode surface. The dielectric constant of the matrix coating, however, will change greatly as it absorbs moisture during the exposure period. The dielectric constant of a typical epoxy is 3.6, and the dielectric constant of water is approximately 80.[15] Therefore, as the epoxy absorbs moisture, the effective dielectric constant will increase.

It may be expected that this moisture uptake and resulting change in τ would also be observed for the unpolarized samples, but polarization has been shown to increase greatly the rate of moisture uptake and ion diffusion into a coating.[16] This can explain why there was no detectable change in τ for the unpolarized specimens.

The fourth noticeable change in electrochemical impedance data is in the Bode magnitude plot. The changes include a decrease in slope and shift of the inclined portion of the curve to lower frequencies. Both of these changes are characteristic of porous electrode behavior and the resulting increase in electrode area. It is also possible that an increase in moisture uptake, as discussed previously, could be partly responsible for the shift of the curve toward lower frequencies. Both of the changes in the magnitude plot translate into an increase in the measured capacitance values.

It is thus apparent that the application of cathodic polarization has a major effect on the electrochemical properties of this graphite/epoxy composite. The impedance data suggest that the composite surface is changing in a way so as to have porous electrode characteristics. Given the insulating nature of the epoxy matrix, this suggests that an increasing amount of graphite fiber is being exposed to solution. This increase of exposed fiber area means that the fiber/matrix interface is being lost, which can result in potential strength losses over time.

Immersion + Cathodic Polarization + Stress

Previous research investigated the effects of cathodic polarization on graphite fiber-reinforced composite materials. Rarely, however, will a functioning composite material operate in an unloaded state.

Figure 18 shows typical impedance data for composite samples that were exposed to all of the environmental conditions (immersion + cathodic polarization + bending stress). The impedance response of these materials includes changes and trends similar to those of the composite samples exposed to immersion and polarization only. Comparison with the data from Figure 16 (immersion + cathodic polarization) reveals no apparent qualitative differences in the impedance spectra.

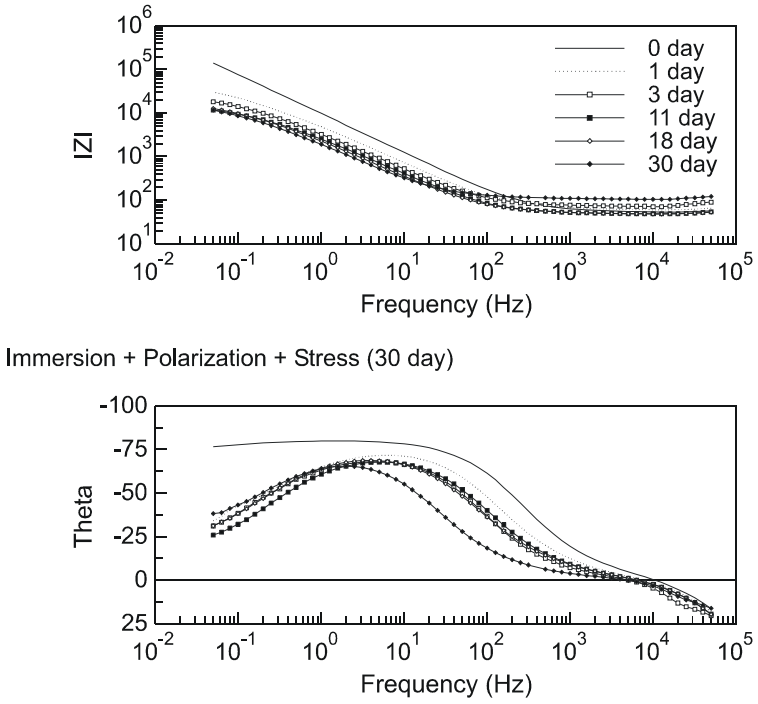

Figure 18. Typical EIS data for a 30-day exposure of gr/epoxy to immersion, cathodic polarization (-1.2 V_{SCE}), and stress (Tank C, No. 8). Impedance magnitude data show increase in capacitance. Phase angle data show drop in R_p after the first day; phase angle peak decreases and curve shifts to left with time. Same trends as seen in Figure 17.

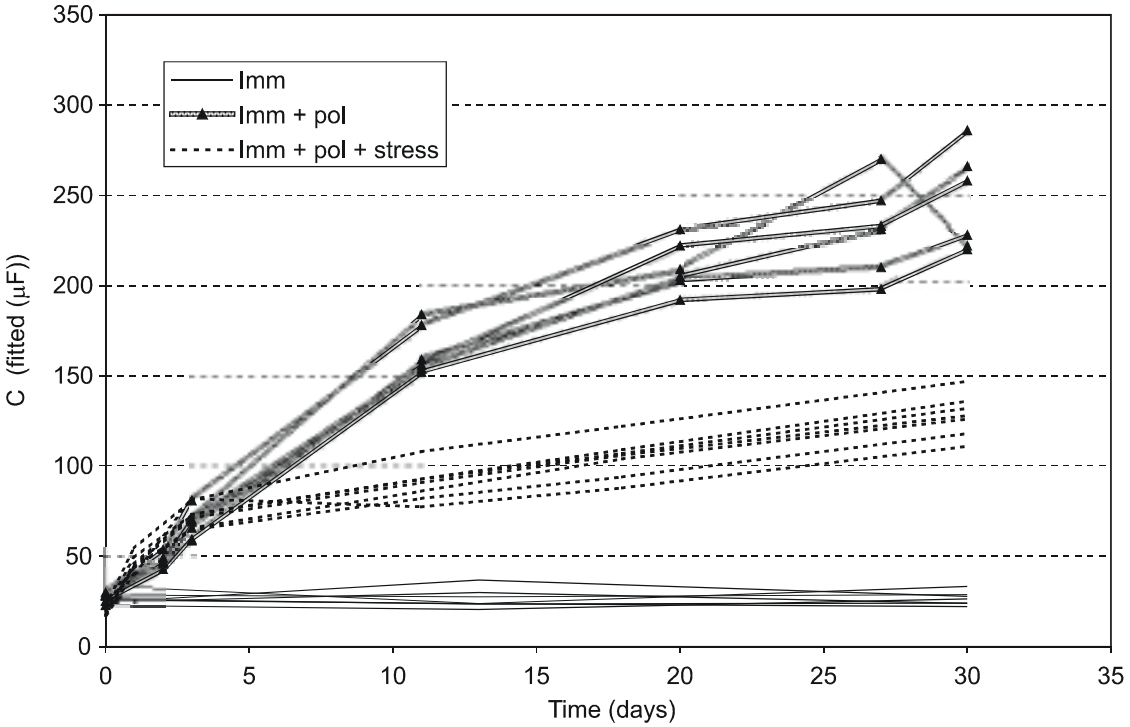

Figure 19. Capacitance values for thick specimen testing (30 days). Values were obtained using an R-CPE circuit.

However, a quantitative analysis of the data using equivalent circuit analogues reveals changes. Figure 19 shows the capacitance values as a function of time for all thick specimen tests. Capacitance values were obtained by modeling the data with a resistor in parallel with a constant phase element (CPE). From the figure, it is evident that capacitance did not increased in the immersed samples whereas it did in both [imm + pol] and [imm + pol + stress] samples. Interestingly, however the application of stress limited the increase in capacitance.

It is not well understood why the application of stress would change the capacitance of the composite. Two mechanisms can be suggested. It may be that the application of stress somehow slows the diffusion of moisture and ions through the epoxy. Slower diffusion could lead to less moisture uptake and thus less of an increase in capacitance. Diffusion of moisture through a polymer is generally associated with the free volume of the polymer. More free volume provides more "space" for moisture to diffuse through. Tensile stress, as occurs on the bottom of the bending samples, is typically assumed to create an increase in free volume, thus enhancing diffusion through a polymer. However, this is not always the case, and some research has shown a slight decrease of free volume for both tensile and compressive stresses for an epoxy.[17] This decrease in free volume could slow moisture uptake into the epoxy, thus resulting in a decreased capacitance compared to the unstressed samples. Another explanation could be that the bending stress is limiting the amount of fiber surface area that is being exposed. The tensile stresses in the epoxy could be resolving into constrictive pressures on the fiber, thus preventing moisture ingress at the fiber/matrix interface.

A model for damage induced by cathodic polarization is suggested by the results of the impedance spectroscopy. The data show the development of porous electrode behavior, which includes an increase in active electrode surface area as evidenced by an increase in capacitance. These are the phenomena that would be predicted for interfacial breakdown between the matrix and fiber, thus allowing for ingress of solution between fiber and matrix.

A possible mechanism for this degradation may be found by examining the overall oxygen reduction reaction:

$$O_2 + 2H_2O + 4e^- \Rightarrow 4OH^-$$

This reaction can proceed by two pathways.[9] The first is the direct four-electron pathway that produces OH^- ions. The other is a potentially much more damaging two-electron pathway that produces reactive peroxide (HO_2^-) species and long-lived superoxide radical intermediates. All of these species produced during the two-electron pathway are able to interact with certain polymer bonds and in many cases degrade a polymer. This pathway is the favored mechanism for oxygen reduction on carbon.

The degradation mechanism may proceed as follows::

1. Oxygen is reduced to hydroxyl ions at the surface of the graphite fibers.

2. Local areas of high pH are generated.

3. The oxygen reduction reaction and high pH in occluded regions near the fibers allows a build-up of peroxide radicals.

4. These reactive peroxide species degrade the polymer matrix in close proximity to the graphite fiber, thus breaking down the fiber/matrix interface.

5. The process continues and as the fiber/matrix bond is lost, solution ingress occurs along the fiber thus inducing a porous electrode response and increasing the active surface area of the electrode.

This mechanism has been proposed by other authors.[4,18,19] Taylor developed an idealized model representing the composite as a cylindrical fiber embedded in an insulating matrix with the fiber axis normal to the composite surface. The “pore” was represented as an annular trench surrounding the fiber, growing deeper into the matrix as damage accumulated.

In the present study, there was no assumption that the pores were V-shaped annular trenches growing downward into the material, as was assumed in previous work.[20] The graphite fibers in the test material are parallel with the sample surface, with only slight undulations. Pore growth proceeds along the fiber matrix boundary, and the depth is limited by the fiber diameter, except in the case where there is connectivity between fiber layers. Consequently, the pores in a more realistic representation of the composite have a more complicated geometry. A schematic of the proposed porous electrode development is shown in Figure 20.

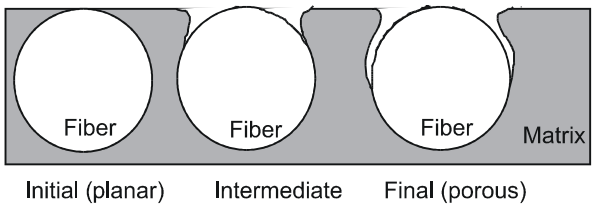

Figure 20. Schematic of porous electrode development for cathodically polarized gr/epxoy composite. Initial composite surface yields planar EIS response. With cathodic polarization, pH increases and matrix is subject to attack of peroxide and superoxide intermediates at fiber/matrix interface. As this continues, interface is lost, allowing electrolyte ingress and porous electrode behavior.

Initially, the composite is assumed to be nominally smooth. Abrasion was performed using 240 grit SiC paper. Typical scratch marks left by this type of paper are on the order of 10 μm. Upon application of cathodic polarization, oxygen is reduced to form hydroxyl species. Since the O_2 reduction takes place on the fibers, local areas of elevated pH develop, possibly in scratch marks, near the fiber/matrix interface. As the pH increases, peroxide species begin to adsorb to the fiber as the two-electron pathway becomes the favored mechanism. The reactive peroxide and superoxide intermediate species produced during these reactions begin to degrade the polymer nearest the interface, as shown by the intermediate stage in the figure. As the matrix degrades, the "pore" that is left behind becomes more occluded, thus allowing for higher pH conditions with increased polymer degradation. As this process continues, the pore depth increases and EIS spectra show porous electrode development, most apparent as a drop in the phase angle.

Figure 21 shows two scanning electron microscopic (SEM) views of the composite surface. Figure 21 (top) is a view of an unpolarized sample. The surface is somewhat rough. More important, the interface between the fiber and matrix is intact. Figure 21 (bottom) is a micrograph of a composite surface that was polarized at -1.2 V_{SCE} for 3 months. Grooves have appeared along the fiber/matrix interface that show a separation of fiber and matrix, and thus loss of interfacial bonding. This micrograph suggests that the porous electrode development is occurring at the fiber/matrix interface and is a result of cathodic polarization.

To determine if the caustic environment created during the reduction of oxygen is sufficient to create the degradation of fiber/matrix interface seen in Figure 21 (bottom), samples were immersed in NaOH solution of pH 13 for approximately 9 months. Figure 22 is an SEM micrograph of the surface after immersion. The figure indicates signs of damage, but this damage is uniform across the entire composite face, much different than the type of damage apparent in Figure 21 (bottom). The figure also shows that the fiber/matrix interface is intact and relatively undamaged. Specimens were also exposed to solutions of pH 1 to pH 13. The surfaces of specimens exposed to these solutions were very similar in appearance, suggesting that the damage seen in Figure 22 is due more to moisture rather than exposure to the specific pH of the solution. This suggests that the intermediates created during the oxygen reduction reaction are responsible for the degradation of the fiber/matrix interface.

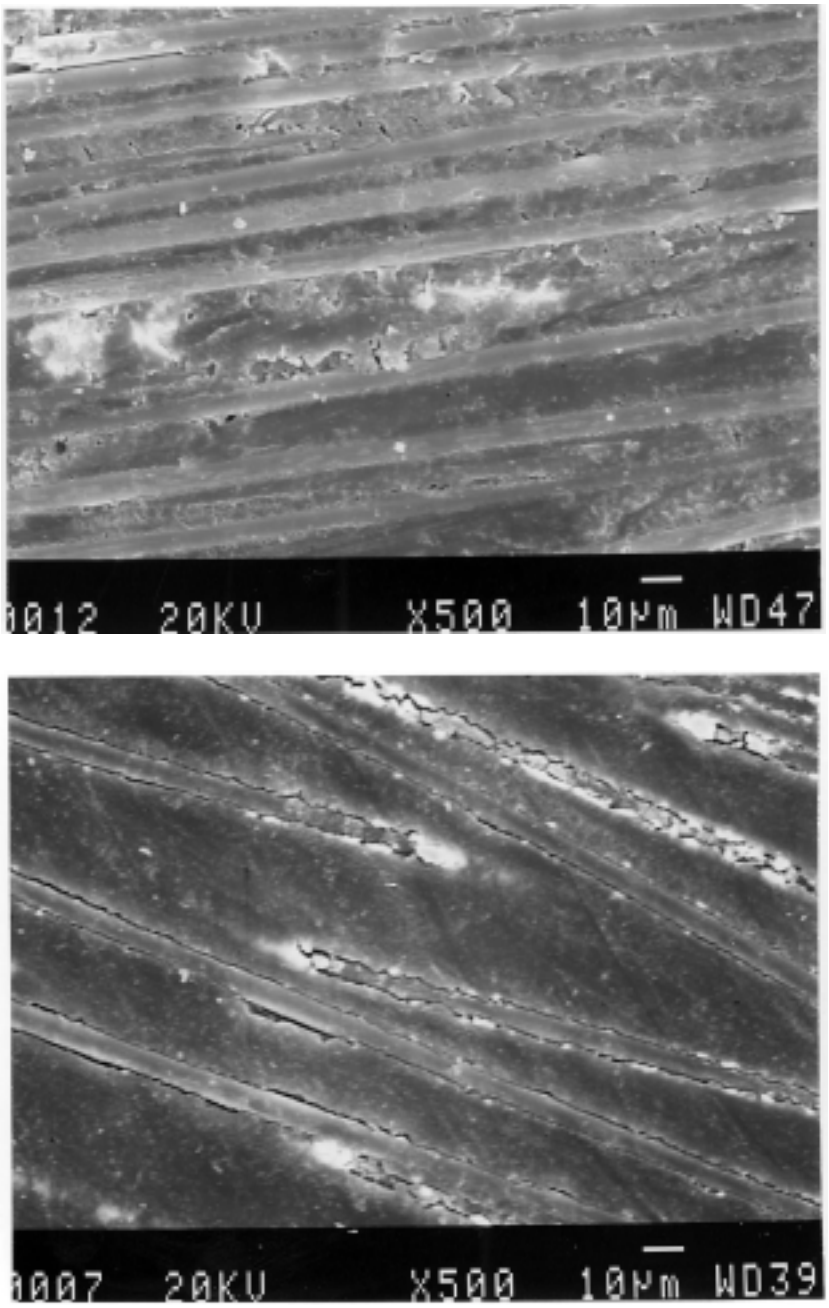

Figure 21. SEM micrographs showing surface of gr/epoxy composite. *Top,* view of unpolarized surface showing good fiber matrix bond. *Bottom,* after 3 months polarization at -1.2 V_{SCE}, grooves have appeared, indicating degradation of fiber matrix interface.

To monitor the development of porous electrode behavior, the value of the phase angle peak was recorded as a function of exposure time. Because of the capacitive nature of the interface and hence negative value of the phase angle, the peak corresponds to the most negative value of phase angle over the scanned frequency range. Figure 23 plots the peak phase angle values verses time for all thick specimen exposures. From the figure, it is apparent that the immersed, unpolarized specimens displayed almost no change in peak phase angle over the

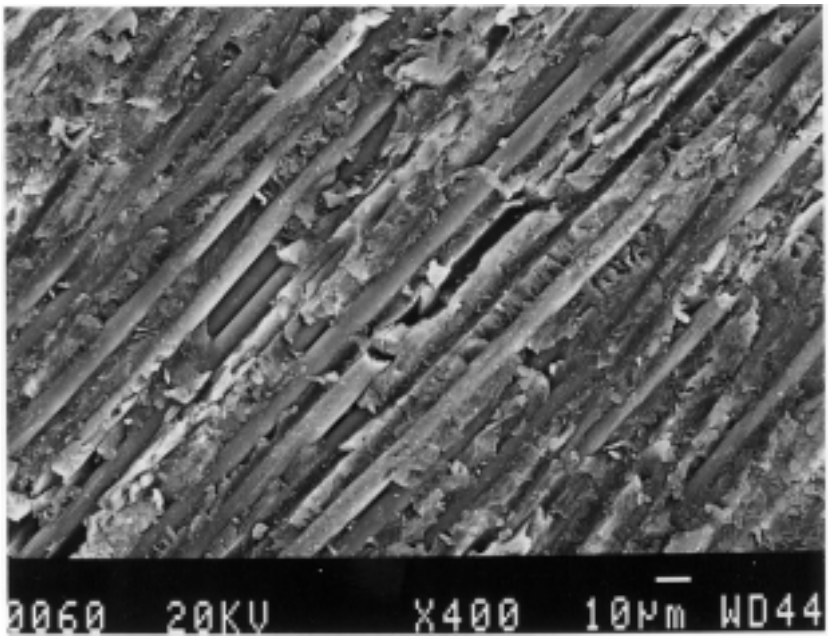

Figure 22. SEM micrograph of a gr/epoxy specimen after exposure to pH 13 solution for 9 months. Interface damage is not apparent.

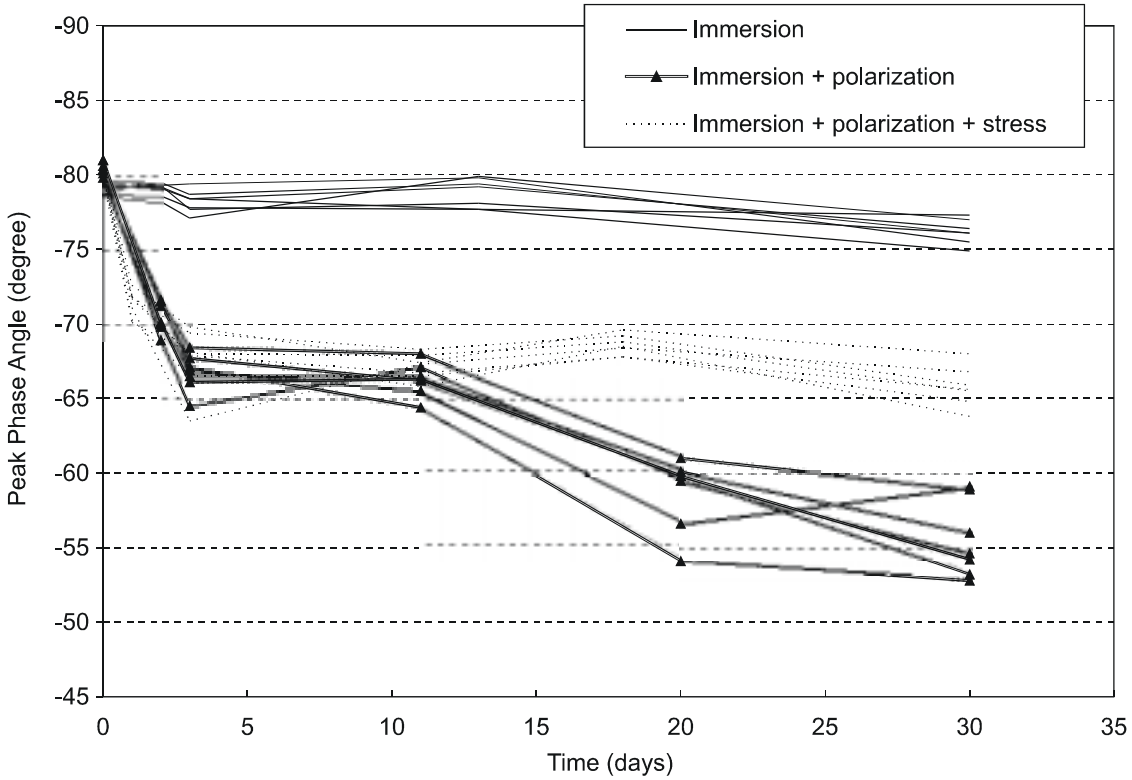

Figure 23. Peak phase angle values for all exposure conditions for thick specimens. Porous electrode development is exhibited as decrease in peak phase angle value.

entire exposure period. At the end of the 30-day exposure, the peak value appears to decrease slightly. This decrease is very small when compared to the changes that are apparent for the other two exposure conditions. A constancy of the peak phase angle value indicates that there is very little, if any, development of porous electrode behavior. This result is consistent with the proposed damage mechanism in that cathodic polarization is required to produce the matrix-degrading species.

The two sets of specimen exposures that included cathodic polarization yielded significant drops in the phase angle peak. The samples exposed to immersion and polarization displayed a continual decrease in peak value over the entire 30-day exposure period. As discussed previously, this drop is indicative of the onset of porous electrode behavior. The samples exposed to the combination of stress + cathodic polarization + immersion display an initial decrease in peak value until Day 10 but do not show a continued drop after. From the figure, it appears that the combination of stress + polarization hinders the continued development of porous behavior. It is also possible the continued development of porous behavior is being masked by some other electrochemical phenomenon. Of major importance is the fact that the impedance spectra were able to reflect the onset of porous behavior long before visual or microscopic detection of composite damage was possible. EIS is a powerful technique and has been demonstrated here and in other studies to be sensitive to the interfacial degradation of graphite fibers in polymer matrices. It has also been used to examine the degradation of organic coatings (paints). It is capable of detecting moisture ingress, microscopic pinholes, and coating/substrate delamination.

If the development of porous electrode behavior, and thus loss of fiber/matrix interface, does indeed lead to a reduction in mechanical strength, these data suggest that the application of stress could decrease the loss in strength caused by the cathodic polarization.

Strength Tests

Figure 24 shows typical load deflection data collected from a bend test of a composite specimen. Load increased linearly with cross head displacement almost until failure. Detectable cracking and “ping” sounds were heard as the specimen neared failure. Failure was sudden and catastrophic. A visible crack grew from the top surface in a downward direction, initiating at the loading point. The crack grew until failure occurred.

Figure 25 is a cumulative probability plot showing the breaking loads for all specimens. This plot shows cumulative probability values on the *y* axis. Load is given on the *x* axis. Breaking load and not stress is reported here. Because of the identical cross-section geometries of all specimens, however, breaking loads from separate tests can be directly compared. The median load can be determined by intersecting the 50 percent cumulative probability with the data for a particular set of tests. From the figure, it is evident that there is much overlap in breaking loads from one exposure condition to the next. Using Student’s *t* test with a confidence interval of 95 percent, it was determined that the results of the strength tests were not statistically significant. The assumption of a Gaussian distribution may not be entirely correct for this material, but it provides a good first order approximation. Thus, the mean values for the exposure conditions did not differ significantly.

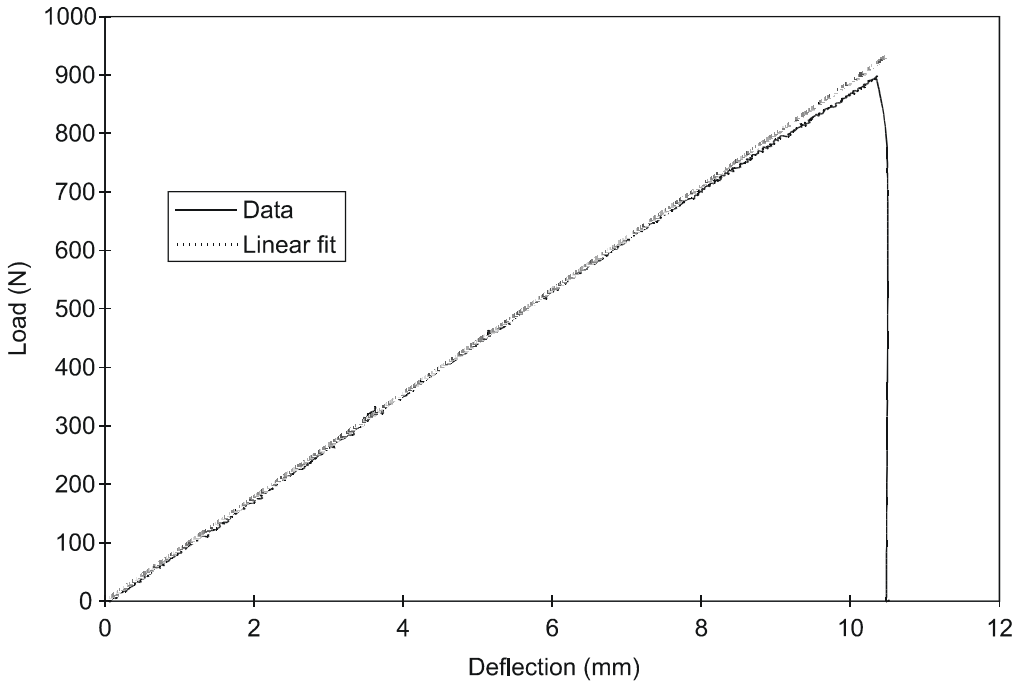

Figure 24. Typical load-deflection data for bend test of gr/epoxy composite (Tank A, No. 6).

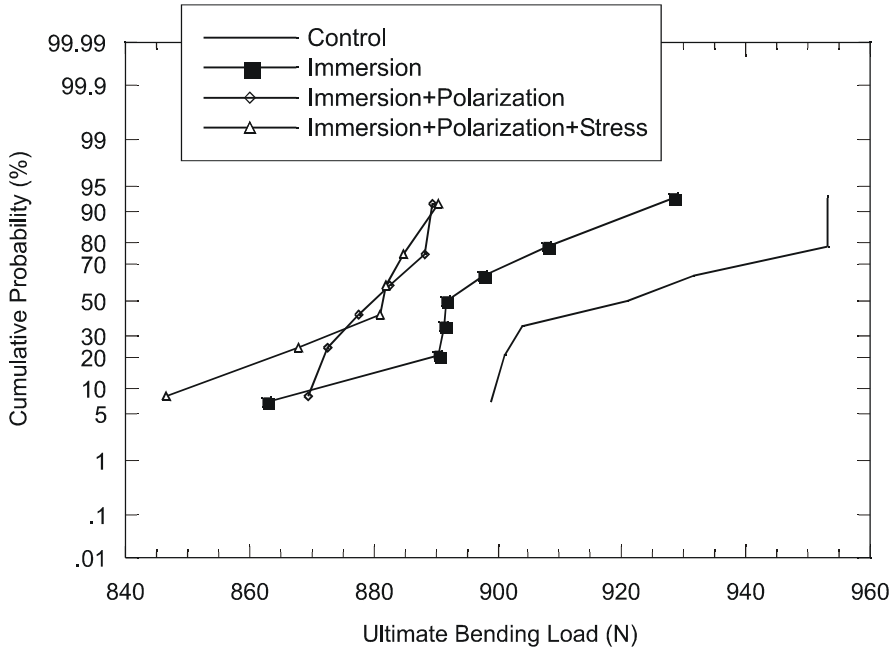

Figure 25. Cumulative probability plot showing distribution of breaking loads for 3-point bend tests of gr/epoxy after 30-day exposures.

Though the strength tests from all exposures showed overlap in breaking load data, very important trends are apparent in Figure 25. From the curves for the control, immersion, and immersion + polarization conditions, it is apparent that the addition of these exposure variables results in a lowering of the breaking load. From investigation of the [imm + pol] and [imm + pol + stress] data, it is apparent that the addition of stress to an applied cathodic polarization does not significantly alter the load at which these composite specimens fail. This result suggests that the differences in porous electrode development discussed previously did not significantly affect the changes in strength data. It should be restated, however, that the changes being discussed are apparent trends and that the strength data for these tests do not indicate statistically significant differences.

Figure 26 shows average values for failure load, deflection at failure, and modulus for the same data shown in Figure 25. For convenience, the data are shown as percentages of the control values. By viewing data in this format, trends in all measured properties are more easily distinguished. From the figure, it can be seen that the average failure load for all exposed samples is lower than that of the control. Average breaking load decreases with increased exposure variables. This drop in failure load is the same result shown in Figure 25 showed. By viewing the data in this format, however, it appears that the addition of stress did slightly depress the average failure load.

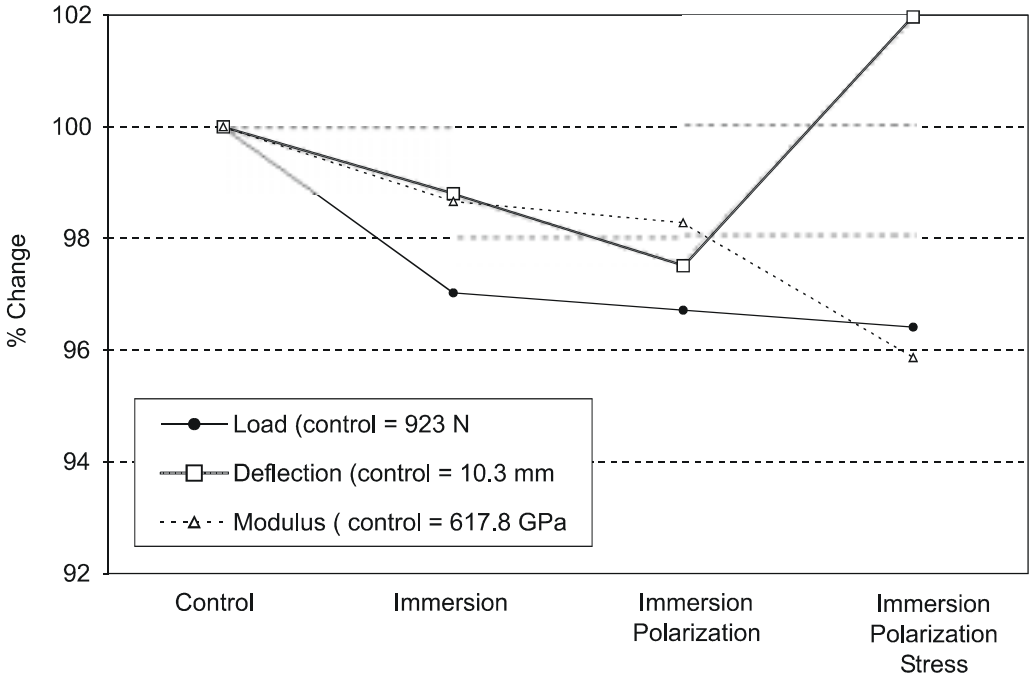

Figure 26. Percentile changes in mechanical testing average data for 3-point bend test of specimens exposed for 30 days. Control samples = 100%.

Average deflections at failure decreased from [control] to [imm] to [imm + pol] samples. However, the samples with combined applications of polarization and stress (i.e., [imm + pol + stress]) showed greater average deflections at failure. All test samples showed a loss of modulus. This is expected because immersion of a polymer typically results in moisture uptake and a decreased glass transition temperature (T_g).[21] The mechanical data for all samples exposed to moisture were only 2 to 4 percent different from the control data, with an undetectable difference between test groups (i.e., [imm] vs. [imm + pol] vs. [imm + pol + stress]). These small changes are well within the experimental scatter of the bend test and expected distribution of composite properties and are therefore not conclusive findings.

Fracture surfaces for composite specimens subjected to three-point bending showed no visible differences between exposure conditions. Each fracture surface revealed a distinct tensile and compressive region. Figure 27 shows typical SEM micrographs of the composite failure surface. The most noticeable surface features are the two distinct zones corresponding to the regions of tension and compression. Figure 27 (bottom) shows a transition region, known as the neutral axis, where the stress state changes from tension to compression. Although the stress distribution is linear through the thickness of a bending sample, the composite fracture surface shows an abrupt change in failure modes.

The roughness of the tensile region was due to individual and clumped fibers protruding from the surface. Figure 28 shows SEM micrographs of these individual and clumped fibers. In both micrographs, the fiber surfaces are very clean. This indicates that the tensile failure was due to fiber pullout. Specimens from each type of exposure condition, including the control specimens, had these same surface features. This failure is also typical of tensile failures of composites with fibers oriented in the loading direction. Upon reaching a critical load, individual fibers fail at a defect in the fiber structure. After the fiber breaks, interfacial stresses increase until the interface also fails, thus allowing the fiber to pull out of the material.[22] The tensile region is very uneven because of the random distribution of fiber-defect locations throughout the composite.

Compressive surfaces revealed terraces of flat fracture surfaces. In these regions, the fibers were fractured evenly with the matrix surface, indicating that the failure mechanism was not that of a fiber pullout or interface failure. This, however, is expected, as fiber pullout requires a tensile stress. These fracture surfaces were created as a crack grew through the thickness of the material. The crack initiated on the top surface at the point of load application. This crack then grew downward, fracturing both the matrix and fiber material. The crack may have been initiated by microbuckling of fibers attributable to the local stress concentration induced by the loading point. This fiber microbuckling was noted as a failure mechanism in other studies using a bend test to study composites with thermosetting matrices.[22-24]

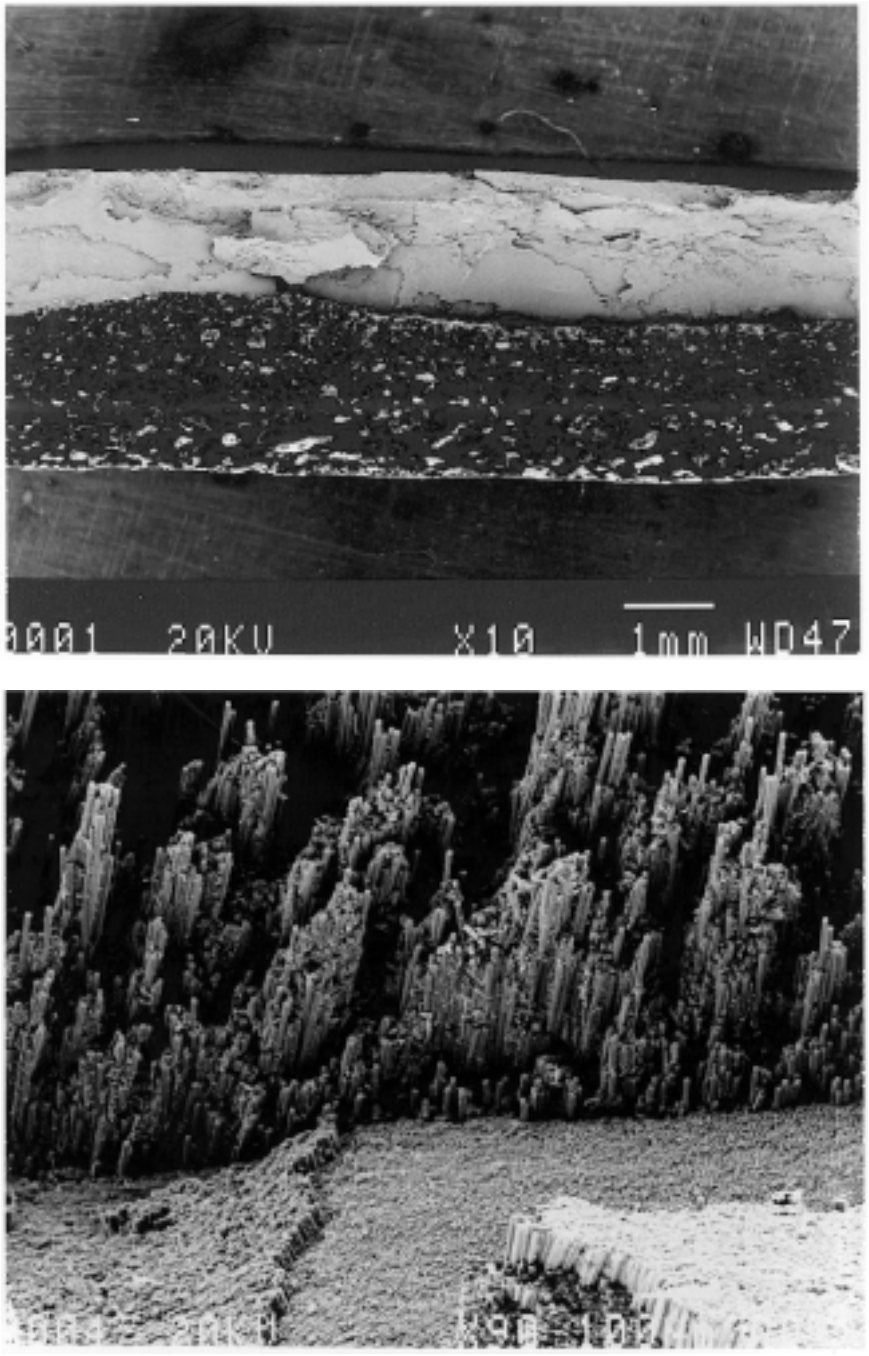

Figure 27. SEM micrographs showing failure surface features for 3-point bend test of gr/epoxy specimens. *Top,* low magnification view of composite surface showing compressive (top) and tensile (bottom) failure regions. *Bottom,* transition from tensile fiber pull-out failure (top, rough surface) to compressive fiber-breakage failure (bottom, smooth terraced ledges) (mag = 90X).

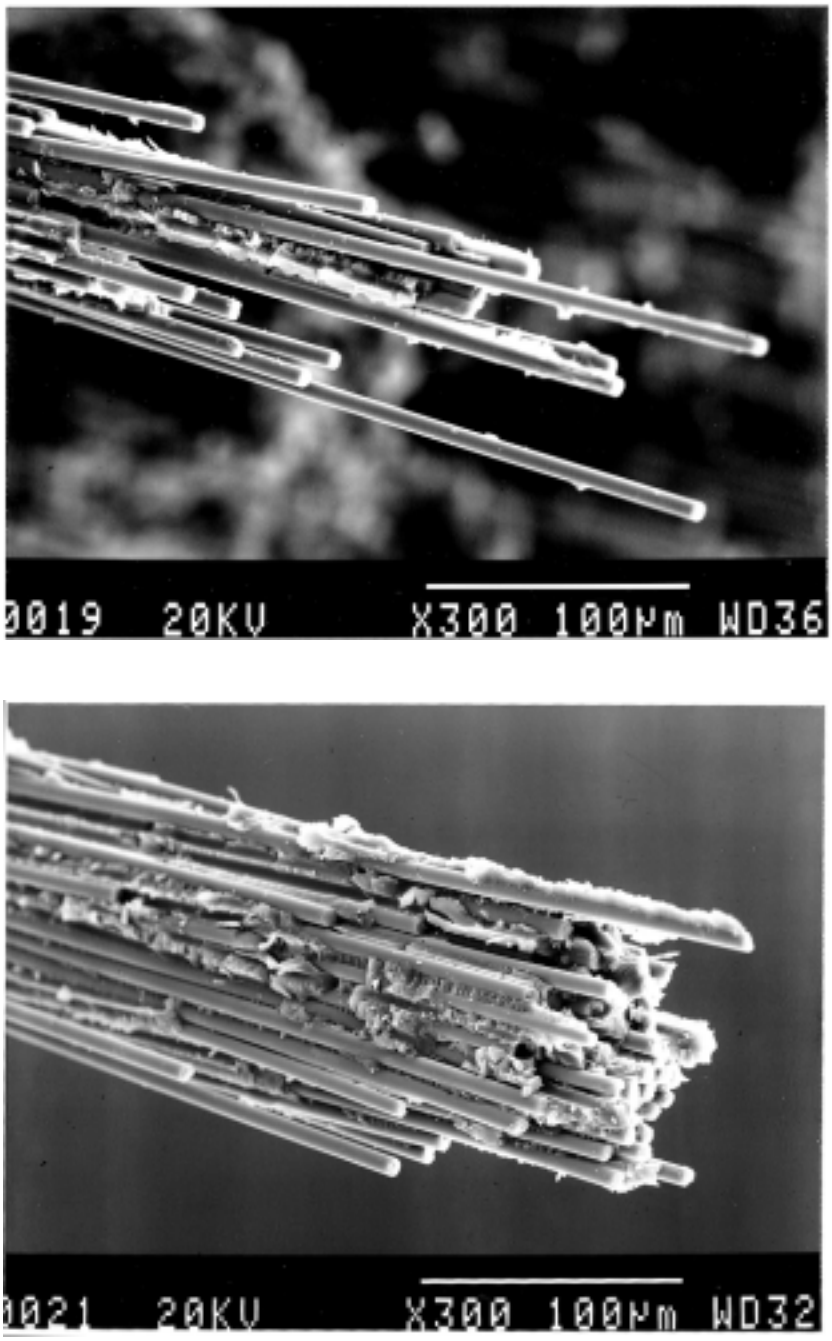

Figure 28. SEM micrographs showing clean fiber surface and fiber pull out for 3-point bend test of gr/epoxy composites. *Top*, fiber pull-out of single fibers. *Bottom*, pull-out of fiber clump.

Summary of Results for Thin Specimens

The results of tests involving thick samples can be divided into EIS (a nondestructive test) results and mechanical testing results. Over a 30-day test, EIS scans showed no change for samples that were only immersed. However, the EIS spectra of specimens exposed to cathodic

polarization and the combination of cathodic polarization + stress showed four changes with time:

1. *A depression of the phase angle at low frequencies.* The depression occurs within 24 hours of exposure and does not continue with exposure. It is possibly due to a change in the end group chemistry of the graphite fiber. This could be a result of either a direct charge transfer reaction or the local increase of pH caused by oxygen reduction. It could also be caused by a slight surface roughening of the electrode.

2. *The apparent development of porous electrode behavior, best evidenced by a drop in the phase angle values between 1 and 1000 Hz.* This behavior is believed to result from the ingress of moisture and hence breakdown of the fiber/matrix interface. This degradation could lead to potentially drastic changes in composite strength over time.

3. *An apparent shifting of the Bode phase angle data toward lower frequencies following extended polarization.* This shift is an indicator that the time constant, τ, is changing and is most likely attributable to differences in reactivity of the freshly exposed fiber surface as porosity is developed. Another possibility a change of the effective dielectric constant of the epoxy "coating" that covers near-surface fibers attributable to polarization-induced moisture uptake.

4. *A tilting of the magnitude curve and a shift to lower frequencies, both signaling an increase in capacitance.* The capacitance values increased for both [imm + pol] and [imm + pol + stress] samples. The application of stress to the polarized samples appeared to limit the capacitance increase. Stressed samples also showed a smaller drop in peak phase angle when compared to [imm + pol] samples, signifying that stress may have slowed the onset of porous electrode behavior.

Mechanical testing of the composite specimens in three-point bending revealed no statistically significant strength losses between exposed or control specimens. Suggestive trends included a decreasing failure load with increased severity of exposure conditions and lower elastic modulus for exposed samples compared to the control. Fracture surfaces for all exposed specimens showed no differences compared to the control surfaces. The region with compressive stresses had a very flat and terraced failure surface that was created by a crack initiating at the loading point and growing downwards until failure. Failure in the tensile region was by fiber pullout.

Thin Specimens

There are four possible reasons the mechanical results were not statistically different:

1. The composite is resistant to strength degradation by the combination of moisture exposure, cathodic polarization, and stress. Thus, no mechanical differences should be observed.

2. The specimen was too thick to allow observation of surface changes that would lead to a degradation of mechanical properties.

3. A 30-day exposure time was not sufficient to create measurable degradation.

4. The three-point bend test was not sensitive to changes in the fiber/matrix interface.

There is support for these possibilities. In a previous study by Sloan and Talbot, damage was observed to occur with the application of cathodic polarization.[18] However, the damage observed was local and only between laminates. The composite material under investigation in this study was pultruded and thus had no laminates.

Other studies on graphite fiber/BMI composites have shown the onset of porous electrode behavior within 24 hours.[20] The longer time required for the onset of porous behavior for graphite/epoxy suggests that the damage is occurring at a much slower rate than for the BMI matrix composites.

Though previous researchers have used a bend test to quantify mechanical properties for composite materials, Cesysson found that the three-point bend test does not give an accurate measurement of the strength characteristics.[6,18,24,25] It is possible that the three-point bend test is not the proper test to quantify fiber/matrix shear strength degradation.

To overcome the uncertainties previously discussed, a thin-specimen testing scheme was designed. The following changes from the thick specimens testing were made:

1. Sample thickness was reduced from 3.32 to ~0.81 mm.

2. Sample exposure time was increased from 30 to 70 days with an additional exposure of 90 days for polarized and polarized + stressed samples.

3. Samples were tested in a Davis test to measure interfacial shear strength between fiber and matrix.

Combined Exposure

The testing scheme included a reduced sample thickness, extended exposure times, and the incorporation of a Davis shear test approach[27] to measure strength changes, as discussed in the Methods section.

EIS Monitoring

Exposure conditions for the thin specimens were identical with those for the thick specimens. The exposure time, however, was increased from 30 to 70 days, with two additional exposures of 90 days for [imm + pol] and [imm + pol + stress] conditions.

Figure 29 shows the Bode phase and magnitude plots for all three exposure conditions: [imm], [imm + pol], [imm + pol + stress] for the 70-day tests. The EIS data show the same trends and changes as for the thick specimens. EIS data for the 90-day exposures were essentially identical as for the 70-day tests.

Figure 29 (top) shows the Bode plots for the graphite/epoxy composite specimens exposed to immersion only. There were no detectable changes in impedance data over the 70-day test. These data suggest that neither the graphite interfacial chemistry nor the fiber/matrix interface of this composite material was affected by immersion in a salt water solution over the time period investigated.

Figure 29 (middle) shows that the addition of an applied cathodic polarization results in changes in the impedance data. The addition of stress to the polarized sample did not produce any additional change in the impedance response. The trends observed in the impedance data were the same as those seen with the thick specimens. The first change was a drop in phase angle at low frequency after 1 day of polarization. This drop indicates a decrease in R_p, signaling that the electrode surface is becoming better able to support a charge transfer reaction. This indicates the possibility of the functional groups on the graphite surface changing in a way to make the material more electrocatalytic, more efficient for an electrochemical reaction. This could enhance the oxygen reduction reaction.

Other changes apparent in the Bode phase angle plot included a decreasing peak phase angle value and a shift of the curve toward lower frequencies with increasing polarization time. As discussed previously, the drop in the phase angle peak is suggestive of the development of porous electrode behavior.[3,4,26] Within the frequency range from approximately 10 to 1000 Hz, the phase angle curve appears to shift to the left, or toward lower frequencies. As discussed previously, this increase in τ could be attributable to a difference in surface reactivity for freshly exposed fibers because of the development of porosity. This freshly exposed fiber surface may be less reactive because of fiber sizing. If this is the case, resistance changes attributable to increased surface area will not be proportional to the actual area change. This would lead to capacitance increases that exceeded the proportional resistance decrease, giving rise to an increase in τ (recall $\tau = R \times C$).

Another reason for the increase in τ, could be an increase in polymer capacitance attributable to the uptake of moisture and ions into the matrix material. This uptake could be accelerated by the cathodic polarization and thus not be evident in the unpolarized samples. As this absorption takes place, the effective capacitance of the epoxy increases because of the relatively high dielectric constant of water compared to the polymer matrix ($\kappa_{water} = 80$, $\kappa_{epoxy} = 3.6$). An increase in capacitance results in a larger τ. As τ increases, the curve will display a shift toward lower frequencies as can be seen in the Bode phase angle plot between 10 to 1000 Hz.

From investigation of the Bode magnitude plots, it appears that the application of cathodic polarization causes a decrease of impedance magnitude in the sloped portion of the curve, resulting in an increased capacitance measurement. Figure 30 shows the capacitance calculated when the electrochemical impedance data were fit to an equivalent circuit analogue

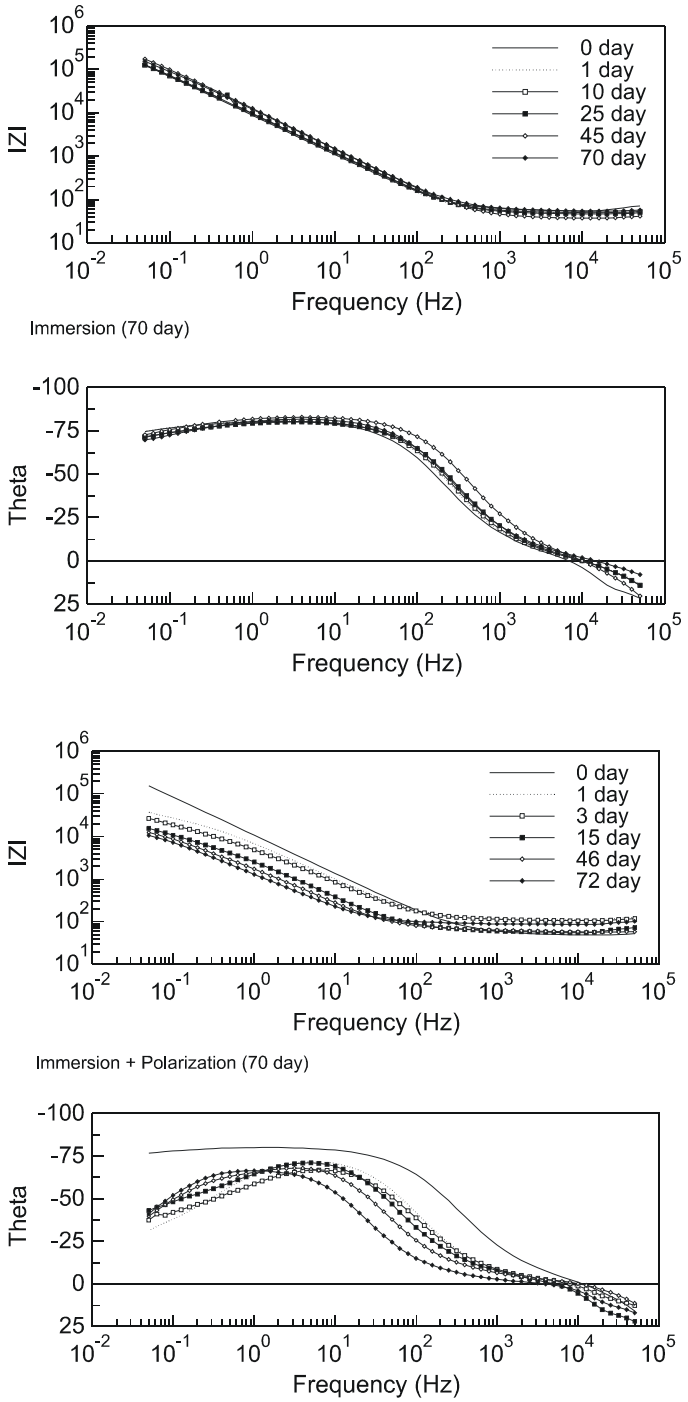

Figure 29. Impedance data for 70-day exposures of thin gr/epoxy composite specimens. *Top two,* data for specimens exposed to immersion in aerated 0.6 M NaCl (sample 6). *Bottom two,* data for immersion + cathodic polarization of -1.2 V_{SCE} (sample 5). *Two on next page,* data for exposure to immersion + cathodic polarization + bending stress (sample 5).

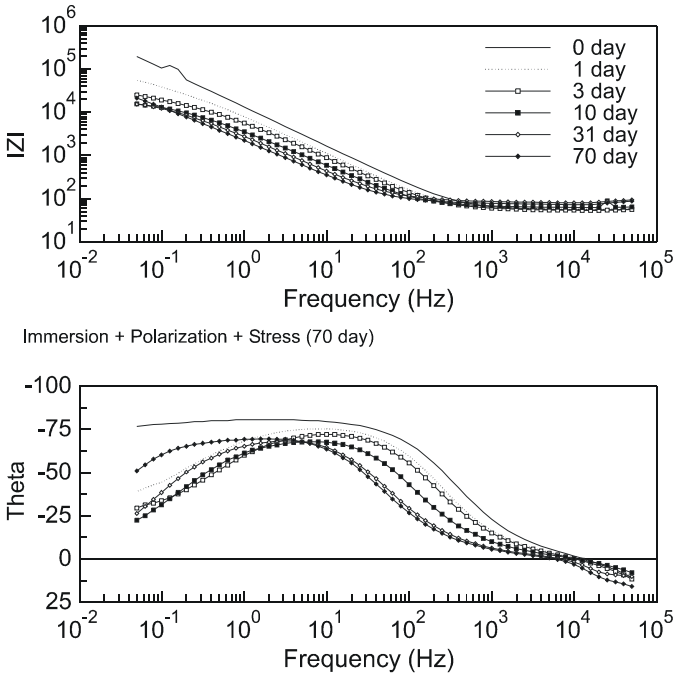

Figure 29 continued.

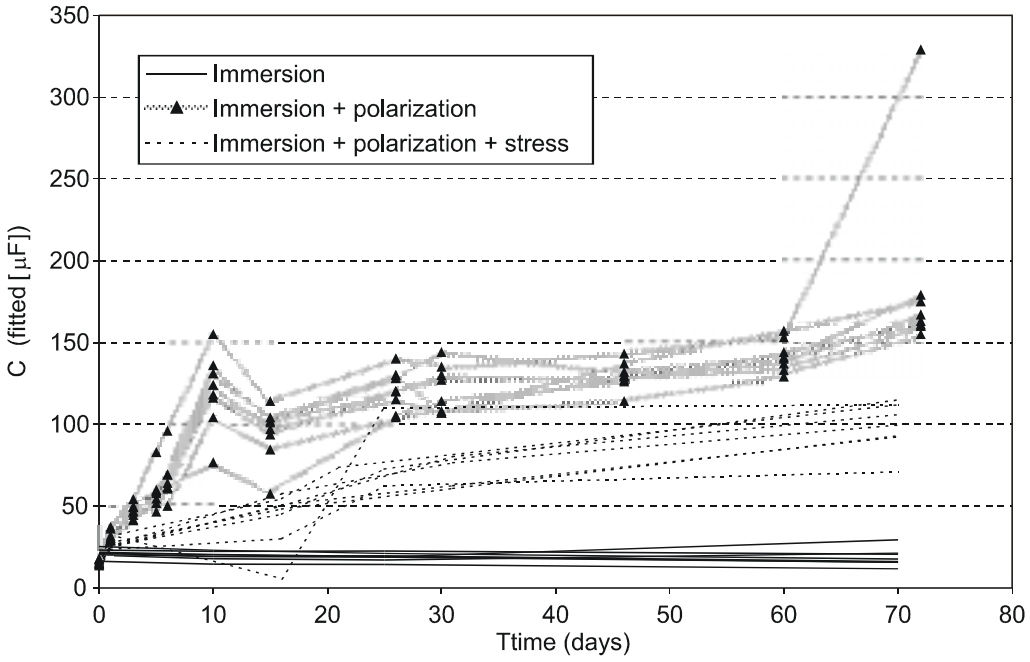

Figure 30. Capacitance values for thin specimen testing (70 days). Values were obtained using R-CPE circuit.

composed of a resistor in series with a CPE (the CPE can be thought of as a non-idealized capacitance that has an adjustable exponent). From the figure, it is evident that the immersed samples did not undergo any capacitance increase whereas both [imm + pol] and [imm + pol + stress] samples underwent increases in capacitance. It is also apparent that the application of stress limits the increase in capacitance. Again, this was the same result seen in the thick specimen testing.

A graphical procedure for monitoring the development of porous electrode behavior was introduced in the discussion of thick specimens (Figure 23). This procedure involved tracking the peak phase angle over the entire exposure period. This procedure was used to monitor the thin specimens also, and the data are shown in Figure 31. There were differences between the data for the thick and thin specimens for the exposure conditions of [imm + pol]. Although the [imm + pol] and [imm + pol + stress] conditions for the thin specimens resulted in similar peak values (-70 degrees) at 70 days, the thick specimens exposed to [imm + pol] displayed a continual drop in peak phase angle, reaching approximately -55 degrees by the end of the 30-day exposure. The thick specimens exposed to [imm + pol + stress], however, showed a leveling of the peak phase angle at approximately -70 degrees, similar to the thin specimens.

A leveling of the peak phase angle does not necessarily mean that the damage occurring on the composite has ceased. Diffusion of moisture and ions into the composite will continue as long as the material is immersed and polarized. It is expected that this will lead to continued degradation of the composite. Damage may be occurring in fiber layers below the surface. However, without a direct electrolyte channel to the next layer, the electrochemical impedance data will show no additional “pore” growth. A direct electrolyte channel can be achieved only if fibers from different layers are in physical contact. If an insulating layer of epoxy exists between fiber layers, there will be no continued growth of the pore and thus no continued development of porous behavior. Though interface damage in subsurface fiber layers may be taking place, it will not be detectable by EIS. This degradation, however, should be apparent in strength data. EIS data should be viewed as a screening method that surveys short-term effects, not necessarily as a method of non-destructive evaluation of long-term exposures.

From Figure 31, it appears that the thin specimens developed porous behavior similar to that of the [imm + pol + stress] samples from the thick specimen testing. It also appears that the addition of stress to the thin specimens slowed the onset of porous electrode behavior, though both exposure conditions yielded similar peak phase angle values after approximately 40 days.

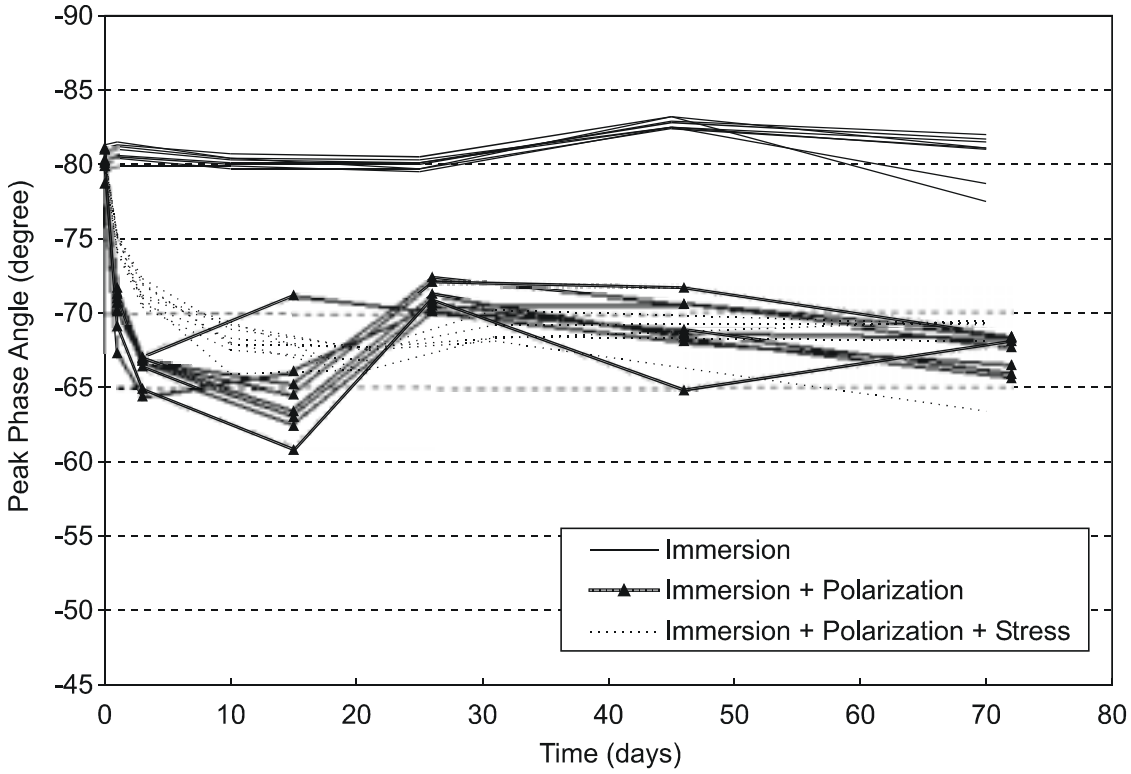

Figure 31. Plot showing peak phase angle values for EIS measurements of thin specimen exposures. Decrease in peak phase angle represents porous electrode development.

Mechanical Testing

Figure 32 shows typical load-displacement data collected for the Davis test. The first noticeable trait is the presence of two load plateaus in the graph. These plateaus are a result of the testing equipment that was used to perform the strength tests. As discussed in the Methods section, testing was carried out on a screw driven loading frame. As with all screw driven machines, there is a small bit of "play" between the driving screws and the loading frame support threads. This small amount of space is the reason for the plateau at approximately 270 N. At a load equal to the weight of the loading frame, the frame goes through a transition from being supported by the loading screws to being forced downward by them. As the screws continue to turn through this transition phase, measured displacement continues to increase though actual displacement remains constant, signified by the plateau. The plateau seen at lower loads (ca. 24 N) is due to the pin in the gripping mechanism not being tightly fit. These two plateaus were seen in all tests at the same load levels and may be disregarded as there is no reason for them to affect ultimate load measurements.

During testing, load increased with cross-head displacement. The figure shows a linear load-displacement relationship before and after the 270 N plateau. This linear behavior, however, was not observed in many of the tests. For this reason, and because strains were not measured, modulus values were not determined for the thin specimen testing. As the specimens neared ultimate load, detectable cracking sounds were audible. With each crack, the load

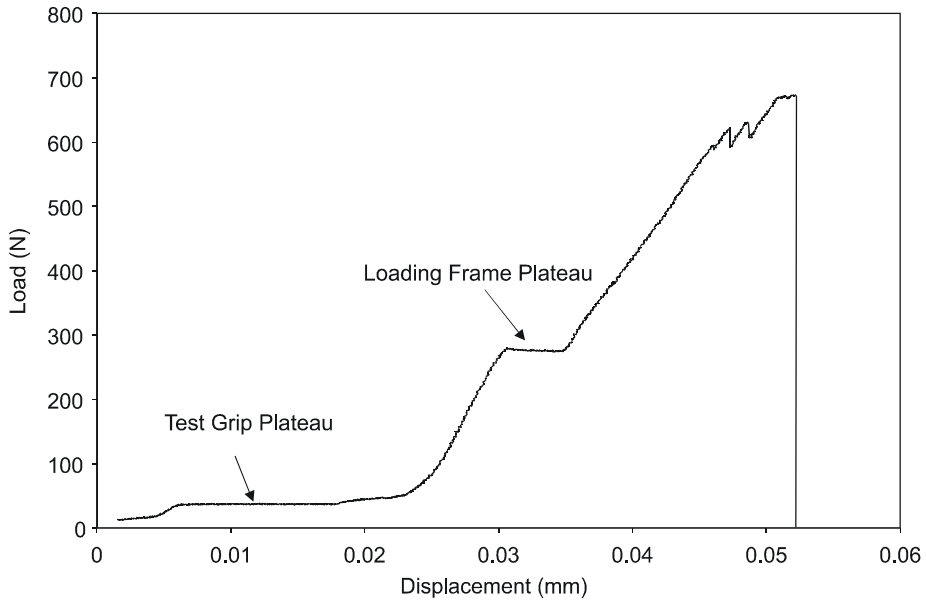

Figure 32. Typical load-deflection data for Davis test of a gr/epoxy composite (imm + polarization + stress, 90 day, No. 6).

Figure 33 shows breaking load data in the form of a cumulative probability plot. It can be seen that there is much overlap in ultimate load data for all specimens. Figure 34 shows the same data as bar graphs. In this figure, the average breaking load value is given for each exposure condition. With each average value, a confidence interval of 95 percent is given. This interval was calculated using Student's *t* test.

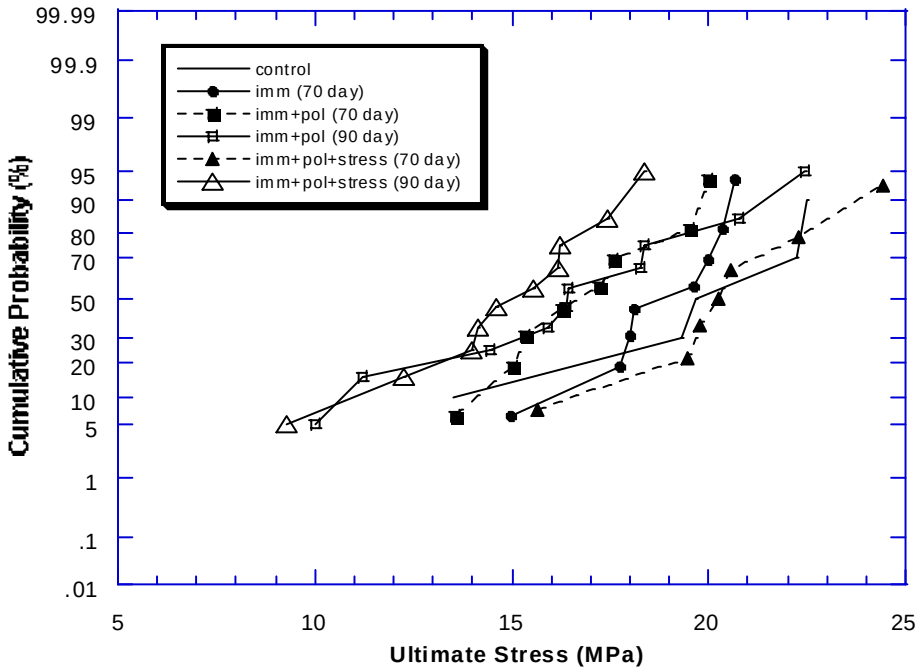

Figure 33. Cumulative probability plot showing ultimate strengths for all gr/epoxy composite specimens tested with Davis test.

From Figure 34, it is apparent that the confidence intervals overlap for all exposure conditions. This indicates that the changes seen in the average data were, as with the bend test data, not statistically significant at the 95 percent confidence level. There are, however, well-defined trends in the average breaking load data that reflect those seen with the thick specimens tested in a three-point bend.

From examination of Figure 34, it is apparent that the average ultimate strength decreased from control to [imm] to [imm + pol] conditions. For exposure conditions [imm + pol] and [imm + pol + stress]), there was a decrease in average strength from Day 70 to Day 90. Another apparent trend for the 70- and 90-day exposures was that the addition of stress to the polarized samples increased the average breaking strength. These changes were not statistically different at the 95 percent level.

It is expected that the average ultimate breaking load would decrease after immersion of a graphite/epoxy specimen. The effects of moisture on the mechanical properties of graphite/epoxy composites have been well studied.[26, 28-33] These studies concluded that diffusion of moisture into the polymer and along the fiber/matrix interface weakens the fiber/matrix bond, resulting in a loss of mechanical properties, especially in those properties dominated by interface strength, such as shear.

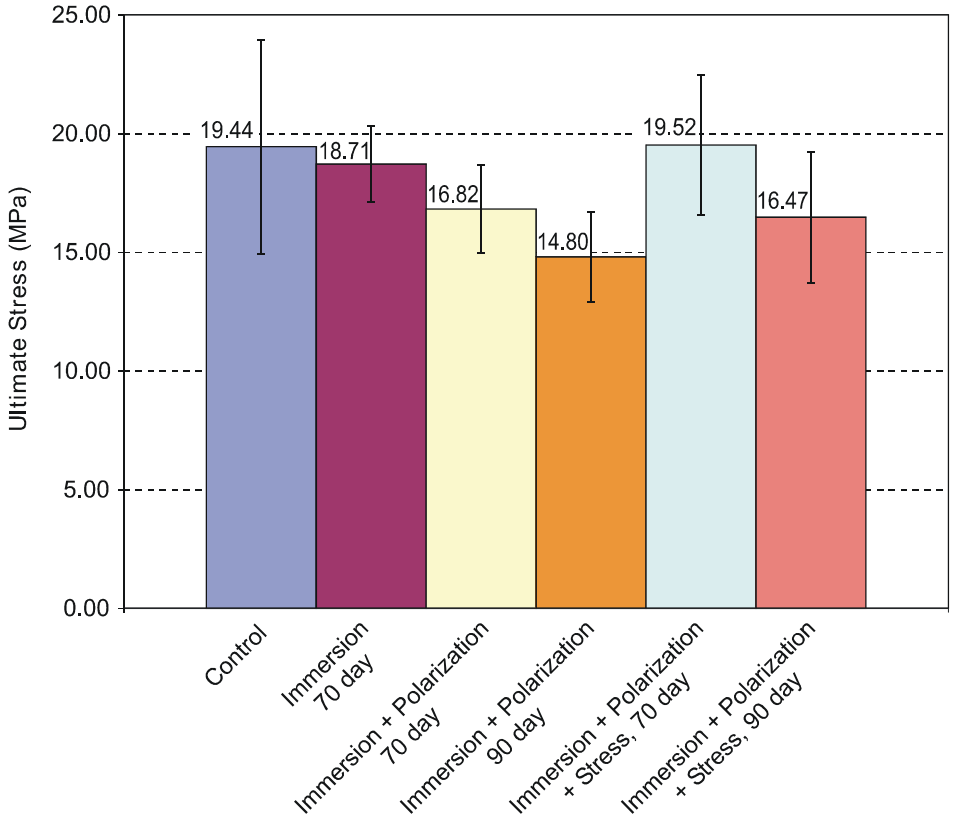

Figure 34. Average ultimate strength values for Davis test specimens. Error bars give 95% confidence interval for mean value.

The application of cathodic polarization to this material would also be expected to result in an increased loss of strength properties, as was seen in the test data. As the fiber/matrix bond is degraded, as evidenced by porous electrode behavior, there is a resulting loss of shear strength. As the length of polarization time is extended, it would be expected that the damage would continue and shear strength would continue to be lost, as is seen when comparing data between 70- and 90-day exposure times. This decrease in average strength over time was seen for both the [imm + pol] and [imm + pol + stress] samples.

The reduction (and possible elimination) in average strength loss caused by the superposition of mechanical stress to cathodically polarized samples was an unexpected result. Though the confidence intervals do overlap slightly between the [imm + pol] (70 day) and the [imm + pol + stress] (70 day) samples, the increase in average strength (actually, absence of strength loss) is the most pronounced result of any of those previously discussed. From Figure 34, it is apparent that the trend is consistent, as the 90-day exposures also show a greater average ultimate strength for the stressed samples when compared to unstressed samples. This increase in strength is also in agreement with EIS phase angle data and measurements of the capacitance. As discussed in previous sections, peak phase angle data were monitored and used as a measure of porous electrode development, and thus degradation of the fiber/matrix interface (Figures 23 and 31). For both the 30-day and 70-day exposures, the stressed specimens appeared to develop a porous response less quickly than the unstressed samples.

Capacitance measurements also provide information about moisture uptake and changes in surface area. Stressed samples showed a smaller increase in double-layer capacitance when compared to unstressed samples (Figures 19 and 31). Capacitance increases can be brought by either moisture uptake by the epoxy or an increase in exposed surface area. Both of these changes are expected to lead to strength degradation, thus a higher strength for the stressed samples. This is in agreement with lower measured capacitance values. As discussed previously, it is not understood why stress would hinder degradative processes for this composite materials. However, both EIS data and strength testing show that there is a beneficial effect of stress in the presence of cathodic polarization. Two theories are presented here as potential explanations for the observed behavior.

One proposed mechanism of how a bending stress could slow strength degradation comes from investigating the transverse effects of bending. Figure 35 shows how a bending stress may result in pore closure on the tensile side of the bent composite sample. In a bent sample, as shown in the figure, compression is developed on the top surface whereas tension is developed on the bottom surface. If the cross section of that sample is examined, the displacements shown in Figure 35b are to be expected when considering a positive Poisson's ratio (Poisson's ratio relates the strain the transverse axes to the strain in the tensile axis). On the compression side, positive transverse strains will be realized, whereas on the tension surface, negative transverse strains are expected. These negative strains may lead to a closing of the grooves that form between fiber and matrix, thus hindering the degradation process. Though an opening of the pores would likewise be expected on the compression surface, it may be that the effects of primary current distribution would make the closing of the pores a more predominant effect, as the tension side is closest to the counter electrode.

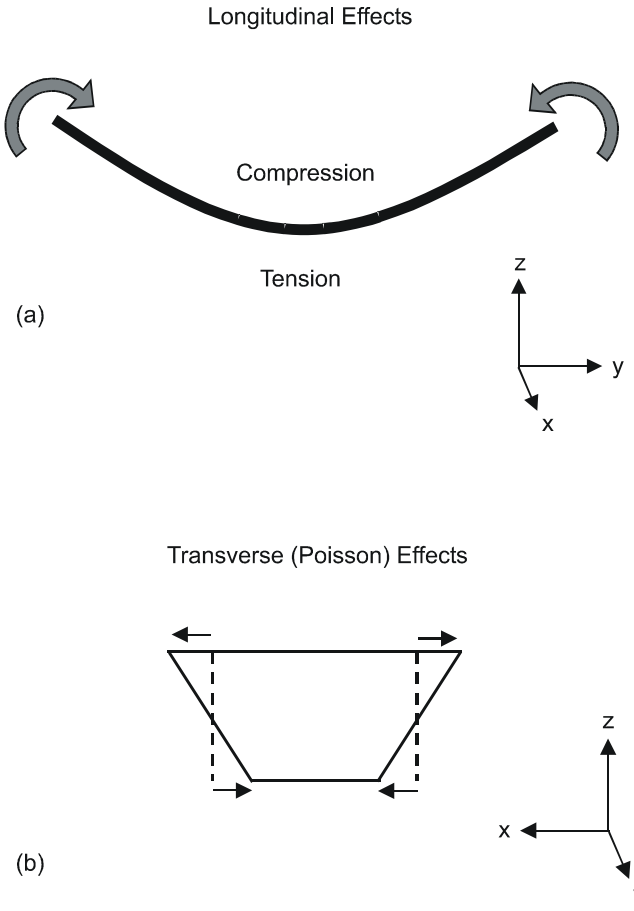

Figure 35. Schematic showing how bending stress may lead to pore closure on tension side of bent specimen, leading to slower degradation rates. (a) Side view showing longitudinal compression and tension on top and bottom surfaces, respectively. (b) End view of bend sample showing positive transverse strains on top surface and negative transverse strains on bottom surface. These negative transverse strains may lead to pore closure and hindrance of strength degradation.

Another mechanism that could hinder the degradation of stressed samples is that the stress slows the diffusion of moisture through the epoxy. As discussed previously, one study concluded that the free volume of epoxies actually decreases under both tension and compression.[17] As diffusion in polymers is typically considered to be a function of free volume, the application of stress would be expected to lead to slower diffusion and thus decreased moisture uptake for the stressed composite samples. However, the effects of stress on diffusion in polymers is controversial, and further work is needed to understand the effect of stress on free volume and thus diffusion in epoxies. Though the mechanism by which the strength degradation is slowed is not well understood, it is evident from both electrochemical testing and mechanical testing that the application of a bending stress to the composite results in a decreased loss of strength when compared to polarized samples that were unstressed.

Examination of the fracture surfaces from the Davis test samples shows the presence of hackles on failure surfaces. Hackles are a classic feature of Mode II, or in-plane shear, fracture.[34] In this type of loading condition, the principle stresses are oriented 45 degrees to the plane of fracture. Brittle matrix fracture occurs normal to this resolved tensile stress, and a series

of distinct microcracks are formed. During fracture, these microcracks coalesce, forming the observed saw-tooth, or hackle, structure. Figure 36 shows a schematic of the Mode II in-plane shear fracture that creates surface hackles.

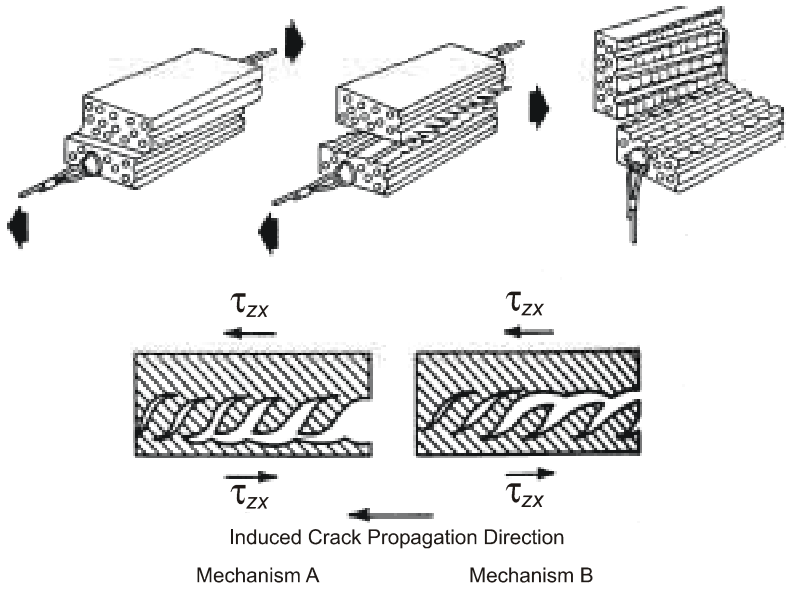

Figure 36. Development of surface hackles on fracture surface of Mode II shear failure.

Figure 37 shows an SEM micrograph of hackles on the failure surface of one of the 70-day immersed thin samples. The presence of hackles indicates a failure of the matrix, not an interface failure, thus signifying strong fiber/matrix adhesion. The presence of hackles has been used by other authors to signify a good fiber/matrix bond.[35-37]

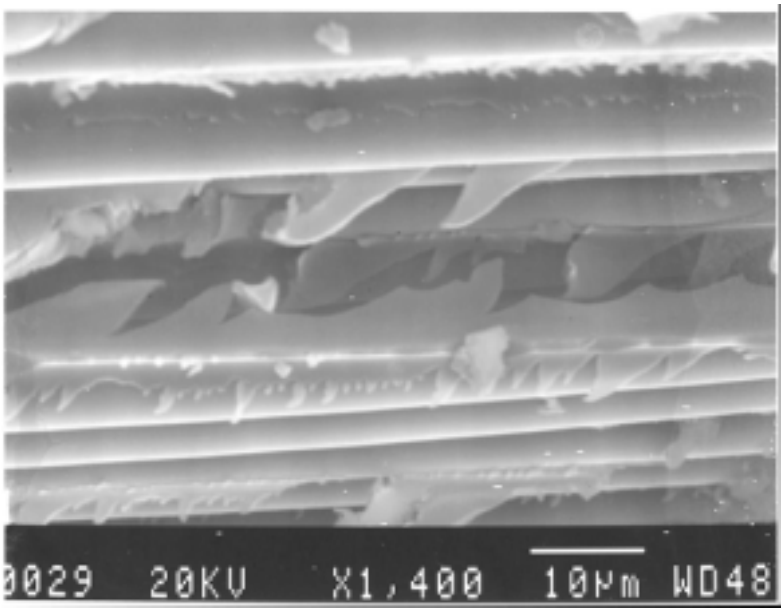

Figure 37. SEM micrograph of hackles on failure surface of gr/epoxy composite exposed to immersion for 70 days and taken to failure in Davis test.

Figure 38 shows SEM micrographs of two thin specimen fracture surfaces near the exposed face of the composite. The top micrograph is of a sample that was immersed for 70 days without polarization. Hackles can be observed on the fracture surface very near the

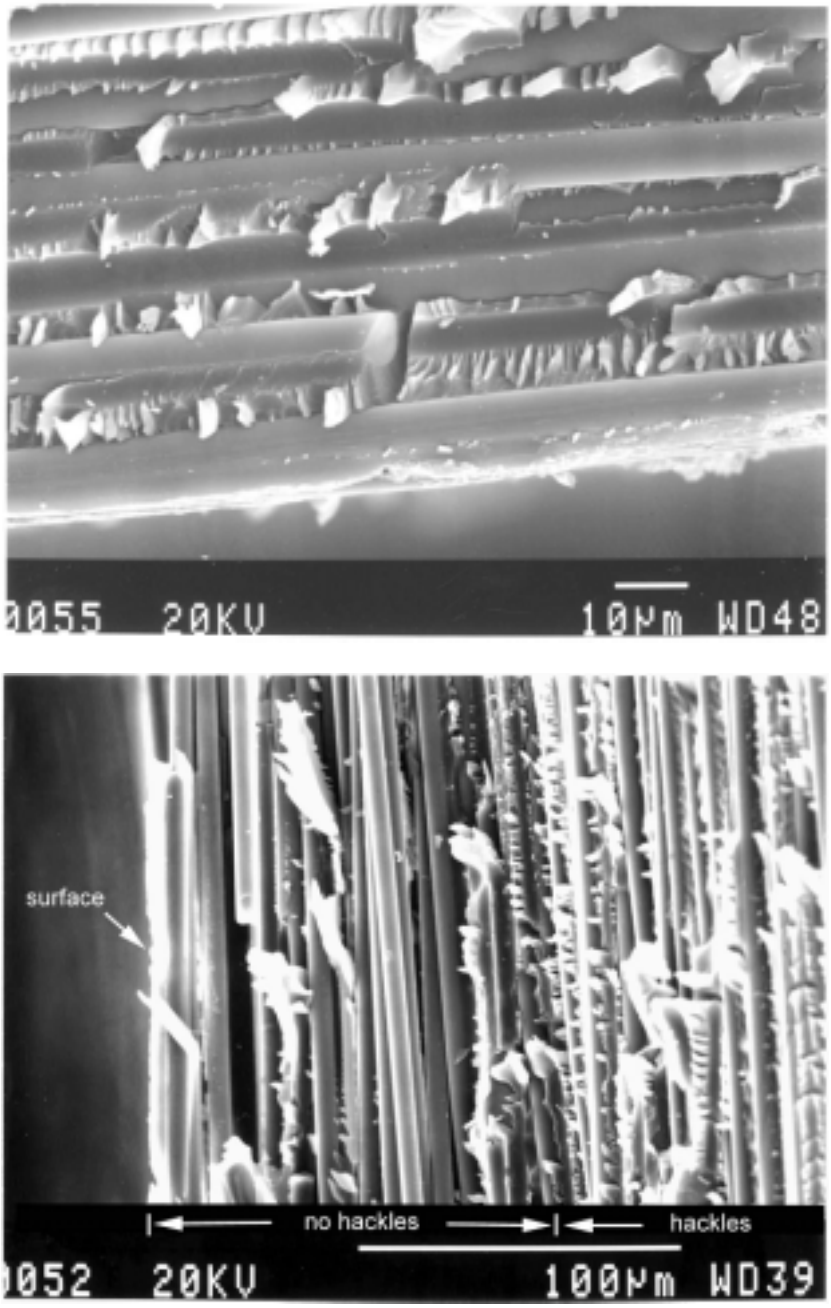

Figure 38. SEM micrographs of fracture surface near exposed face of gr/epoxy composite thin specimens. *Top,* specimen exposed to immersion for 70 days. Notice hackles beginning immediately below exposed face. *Bottom,* specimen exposed to cathodic polarization and stress for 90 days. Fiber surfaces near exposed face (within ca. 100 μm) show no hackles because of polarization-induced damage.

exposed face. The bottom micrograph shows the edge of a sample that was exposed to [imm + pol + stress] for 90 days. It is evident that there are no hackles near the exposed face of the composite. The hackle formation does not begin until approximately 100 μm away from the composite face, indicating that the fiber/matrix interface damage had penetrated at least 100 μm into the composite over the 90-day period.

Figure 39 is an SEM micrograph taken of the composite face of the same specimen as shown in Figure 38 (bottom). It is apparent that the fiber/matrix interface of the surface fibers has been badly damaged. It is expected that with time and moisture ingress, this damage could penetrate deeper into the composite. These hackle-free zones support the notion that the polarization-induced damage is able to penetrate the surface of the material. Taylor observed hackles on fracture surfaces of a graphite fiber/BMI composite tested using a Davis test.[36] Hackles were observed in all specimens except those exposed to cathodic polarization. These polarized specimens showed no hackles across the entire cross section, signifying that fiber/matrix damage had taken place through the entire thickness of the composite. It should be noted that BMI polymers are very susceptible to alkaline attack.

SEM investigation of all exposure conditions that included cathodic polarization showed failure surfaces similar to the one in Figure 38. The damage zones for these specimens, indicated by no hackles, ranged from 30 to 120 μm in depth. Penetration values were difficult to calculate because hackle-free zones continually ranged in breadth over the entire specimen. All investigated specimens that were exposed to cathodic polarization appeared to have similar amounts of damage. The composite surface that faced that counter electrode showed deeper

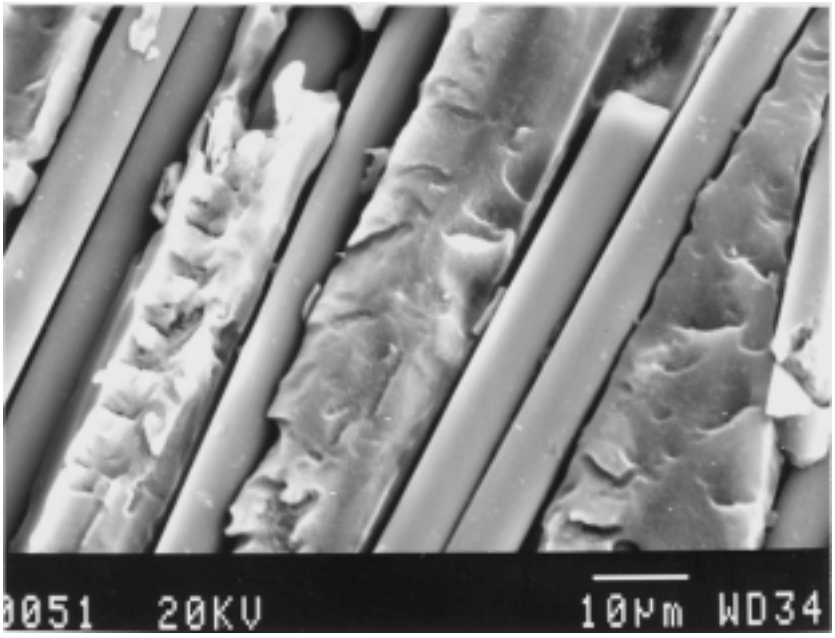

Figure 39. SEM micrograph of exposure face of thin specimen exposed to immersion + polarization + stress for 90-day period. Notice lack of fiber matrix interface integrity.

damage. This was expected as current density will be higher for these faces because of primary current distributions associated with the cell geometry (i.e., this face is closer to the counter electrode).

If an average damage penetration depth is approximately 50 to 70 μm after exposure times of 70 to 90 days, the result is a 10 to 15 percent decrease in cross-sectional surface area for a sample 1 mm thick by 10 mm wide. Thus, it would be expected that the polarized samples would show a 10 to 15 percent strength loss when compared to the immersed samples. Using the average strength values from the Davis testing (Figure 34), the strength losses were calculated and are shown in Table 2.

Table 2. Percentage Decrease in Average Ultimate Strength As Result of Adding Applied Cathodic Polarization of -1.2 V_{SCE}

Test Condition	Average Ultimate Strength (MPa)	Strength Decrease (%)
Immersed (70 day)	18.71	---
Imm + pol (70 day)	16.82	10.1
Imm+ pol (90 day)	14.8	20.9
Imm + pol + stress (70 day)	19.52	N.A.
Imm + pol + stress (90 day)	16.47	12.0

Correlation of strength loss with loss of cross-sectional area yields acceptable agreement when consideration for data scatter is taken into account. This correlation is a rough estimate using average strength values from data that do not show statistically significant trends. Strength losses for all but the [imm + pol + stress] 70-day tests show acceptable correlation with cross-sectional area changes. Correlation is not made with these samples because of the increased strength that is apparent from the testing data.

The strength loss by pultruded specimens is consistent with strength losses in graphite/epoxy composites from other studies. Sloan and Talbot studied damage induced from galvanic couples of graphite/epoxy to magnesium in seawater for 140 days.[18] Strength losses of approximately 30 percent were measured. However, damage penetration rates were very high (6 to 8 mm/yr) in this study. Assuming an average penetration of 50 to 70 μm after 70 days for the pultruded specimens in the present study, penetration rates were only 0.2 to 0.3 mm/yr more than an order of magnitude less than in the Sloan and Talbot study.[18] The reason for this difference comes from the fabrication method used to produce the specimens for each study. Sloan and Talbot studied a laminated composite consisting of 26 plies, where the present study investigated

a pultruded composite with no laminates. In their study, delamination damage appeared to be localized, beginning at the composite edge and extending inward along the laminate interface. This localized delamination of the plies was the cause of the observed high strength loss. The damage noted for the pultruded specimens was more a general penetration of moisture and interfacial degradation, beginning at the composite face and penetrating inward.

Laminated composites have an inherent weakness: the laminate interface. These boundaries are more susceptible to moisture attack than the actual laminate material, as noted by Sloan and Talbot. Pultruded samples are essentially a single laminate, and thus there are no laminate interfaces present for localized moisture ingress and attack. Without localized attack, damage is more uniform across the composite face, leading to lower penetration rates.

It is important to note, however, that though damage rates were much lower in the present study, relative strength losses between the Sloan and Talbot study and this study are comparable. The former study used a four-point bend test to determine strength losses, whereas the present study incorporated a Davis shear test.[18]

Summary of Results for Thin Specimens

The EIS monitoring for both the 70- and 90-day exposures showed the same changes as for the thick specimens. EIS scans for the immersed samples that were under no applied polarization showed no change in the EIS spectra. Specimens exposed to [imm + pol] and to [imm + pol + stress] exhibited similar changes over the exposure period:

- a dramatic decrease in R_p after the first 24 hours of exposure
- a drop in peak phase angle
- an increase in the time constant
- a decrease in the impedance magnitude with time.

After exposure, the specimens were tested to failure using a Davis shear test. The differences in observed mechanical strengths were not statistically significant, but trends can be seen in the data. These trends include a decrease in ultimate strength from the exposure conditions of control to [imm] to [imm + pol]. For the [imm + pol] specimens, a 90-day exposure showed reduced ultimate loads when compared with a 70-day exposure. The addition of stress to polarized samples prevented this loss in ultimate strength. The 90-day exposure yielded a lower ultimate breaking load than the 70-day exposure.

Hackles were observed in the failure surface, indicating a mode II in-plane shear failure. For all exposures that included cathodic polarization, a hackle-free zone of 30 to 120 μm was apparent near the exposed face of the composite, indicating fiber/matrix interface degradation. Penetration calculations reveal a 10 to 15 percent decrease in cross-sectional area, corresponding well with the 10 to 20 percent decrease in average strength observed for [imm + pol] specimens

when compared to immersed samples. The decrease in cross-sectional area was also observed for [imm + pol + stress] samples, but reductions in strength were not seen in the 70-day exposure time for these conditions. The 90-day exposure period for [imm + pol + stress] samples showed an approximate 20 percent loss in strength when compared to immersed samples, also agreeing well with the approximate 10 to 15 percent loss of cross-sectional area.

SUMMARY OF RESULTS

The findings of this study indicate that graphite/epoxy composites cannot be assumed to be insensitive to degradation by environmental variables. Further, electrochemical polarization, as might occur with contact with a metal such as a fastener, can accelerate degradation. This damage requires the presence of moisture. Chloride and sulfate concentrations in rain are sufficient to establish an electrolyte within creviced regions, but deicing salts would overtake these as a contributor to conductivity.

Further results may be summarized as follows:

- Immersion of composites up to 90 days in 0.6M NaCl does not result in any change in the EIS spectra.

- Application of polarization in an aerated 0.6M NaCl environment leads to breakdown of the fiber/matrix interface. The high pH environment created during the oxygen reduction reaction is necessary but not sufficient to create this breakdown, as the unpolarized specimen exposed to a pH 13 environment did not degrade. Cathodic polarization as would occur by coupling to steel or aluminum is required.

- Application of cathodic polarization does not significantly alter strength. Average measurements of shear strength, however, did show a decrease with the application of cathodic polarization for 70 and 90 days.

CONCLUSIONS

- EIS can detect changes in composite surface morphology (porous electrode behavior), which signals a breakdown of the fiber/matrix interface, and changes in end-group chemistry of the graphite fiber.

- EIS is not able to detect continued penetration of fiber/matrix damage after approximately 40 days because of the lack of a continuous electrolyte channel to these subsurface layers.

- Longer exposure times increase average strength loss.

- Application of stress in combination with cathodic polarization appears to increase the average strength of the composite, relative to polarization without stress.

- Average damage penetration rates for this pultruded composite are much lower than for laminated composites. The lack of laminate interfaces is beneficial in preventing the localized attack that has been observed in laminated graphite/epoxy composites.

- Before widespread incorporation of carbon fiber composites can be realized in the infrastructure, a more accurate understanding of the environmental effects on strength durability is needed.

RECOMMENDATIONS FOR FURTHER STUDY

- Include longer exposure times and a larger sample size for this graphite fiber/epoxy composite in an attempt to obtain statistically significant strength changes.

- Test composites under conditions of stress + no polarization to understand the mechanism by which stress slows strength degradation. In addition, investigate the effects of tensile stresses, both monotonic and cyclic.

- Study the effects of anodic overpotentials to simulate possible stray current polarizations that are possible in the field.

- Test in simulated pore solution and in actual concrete to achieve an environment more representative of field conditions if composites are to be incorporated into concrete structures (e.g., rebar, prestressing tendons).

- Preliminary electrochemical testing showed that state-of-the art graphite fiber/epoxy composites have similar electrochemical properties and show the same initial response to cathodic polarization as this tested material, suggesting that investigation of the long-term effects of cathodic polarization of these materials should be carried out before incorporation into the infrastructure.

REFERENCES

1. U.S. Secretary of Transportation. *1995 Status of the Nation's Surface Transportation System: Condition and Performance: Report to the United States Congress.* U.S. Government Printing Office, Washington, D.C., 1996.

2. Tucker, W.C., Brown, R., and Russell, L. Corrosion Between a Graphite/Polymer Composite and Metals. *Journal of Composite Materials,* Vol. 24, 1990.

3. Wall, F.D., Taylor, S.R., and Cahen, G.L. The Simulation and Detection of Electrochemically Derived Damage in Bismaleimide/Graphite Fiber Composites. *ASTM STP 1174, High Temperature and Environmental Effects on Polymeric Composites,* C.E. Harris and T.S. Gates, eds. American Society for Testing and Materials, Philadelphia, 1993.

4. Taylor, S.R., Wall, F.D., and Cahen, G.L. The Detection and Analysis of Electrochemical Damage in Bismaleimide/Graphite Fiber Composites. *Journal of the Electrochemical Society,* Vol. 143, No. 2, 1996.

5. Herakovich, C.T., and Mirzadeh, F. Properties of Pultruded Graphite/Epoxy. *Journal of Reinforced Plastics and Composites,* Vol. 10, 1991.

6. Ceysson, O. Creep Damage Characterization of CFRP Laminates. In *Progress in Durability Analysis of Composite Systems: Proceedings of the International Conference on DURACOSYS 95,* A.H. Cardon, H. Fakuda, and K. Reifsneider, eds. A.A. Balkema, Rotterdam, The Netherlands, 1996.

7. Taylor, S.R., Stewart, K.C., and Cahen, G.L. *The Detection and Analysis of Electrochemical Degradation in High Temperature Polymer Matrix Composites.* Contract No. N62269-92-M-3271. University of Virginia, School of Engineering & Applied Science, Charlottesville, 1993.

8. Randin, J.P. Carbon. In *Encyclopedia of Electrochemistry of the Elements,* Vol. VII, A.J. Bard, ed. Marcel-Dekker, New York, 1976.

9. Yeager, E., Molla, J.A., and Gupta, S. The Electrochemistry of Carbon. In *Proceedings of the Electrochemical Society,* Vol. 84-5, Philadelphia, 1984.

10. Mattson, J.S., and Mark, H.B. *Activated Carbon*. Marcel Dekker, New York, 1971.

11. Stafford, G.R. Graphite Fiber-Polymer Matrix Composites as Electrolysis Electrodes. *Journal of the Electrochemical Society,* Vol. 138, No. 2, 1991.

12. de Levie, R. On Porous Electrodes in Electrolyte Solutions. *Electrochimica Acta,* Vol. 8, 1963.

13. de Levie, R. On Porous Electrodes in Electrolyte Solutions IV. *Electrochimica Acta,* Vol. 9, 1964.

14. de Levie, R. The Influence of Surface Roughness of Solid Electrodes on Electrochemical Measurements. *Electrochimica Acta,* Vol. 10, p. 113, 1965.

15. Hodgman, C., ed. *Handbook of Chemistry and Physics.* Chemical Rubber Publishing Co., Akron, Ohio, 1955.

16. Schwenk, W. Adhesion Loss of Organic Coatings: Causes and Consequences for Corrosion Resistant Coatings. In *Corrosion Control by Organic Coatings*, H. Leidheiser, Jr., ed. National Association of Corrosion Engineers, Houston, Texas, p. 103, 1981.

17. Young, R.J., and Lovell, P.A. *Introduction to Polymers*, 2nd ed. Chapman & Hall, New York, 1996.

18. Sloan, F.E, and Talbot, J.B. Corrosion of Graphite-Fiber-Reinforced Composites I: Galvanic Coupling Damage. *Corrosion*, Vol. 48, No. 10, 1992.

19. Taylor, S.R., and Cahen, G.L. *The Detection and Analysis of Galvanic Damage in BMI/Graphite Fiber Composites.* Presented at AGARD Structures and Materials Panel on Corrosion Detection and Management of Advanced Airframe Materials, p. 6-1, 1995.

20. Taylor, S.R. A Nondestructive Electrochemical Method to Detect and Quantify Graphite Fiber/Polymer Matrix Disbondment in Aqueous and Cathodically Polarized Conditions. *Composite Interfaces*, Vol. 2, No. 6, 1994.

21. Schwartz, M.M. *Composite Materials: Volume I: Properties, Nondestructive Testing, and Repair.* Prentice Hall, Newark, N.J., 1996.

22. Karayaka, M., and Kurath, P. Deformation and Failure Behavior of Woven Composite Laminates. *Journal of Engineering Materials and Technology*, Vol. 116, 1994.

23. Miyano, Y. Long Term Prediction Method for static, Creep and Fatigue Strengths of CFRP Composites. In *Progress in Durability Analysis of Composite Systems: Proceedings of the International Conference on DURACOSYS 95,* A.H. Cardon, H. Fakuda, and K. Reifsneider, eds. A.A. Balkema, Rotterdam, The Netherlands, 1996.

24. Whitney, J.M., and Husman, G.E. Use of the Flexure Test for Determining Environmental Behavior of Fibrous Composites. *Experimental Mechanics*, Vol. 4, No. 18, 1978.

25. Gomez, J.P., and Casto, B. *Freeze-Thaw Durability of Composite Materials.* VTRC 96-R25. Virginia Transportation Research Council, Charlottesville, 1996.

26. Loos, A.C., and Springer, G.S. Effects of Thermal Spiking on Graphite-Epoxy Composites. In *Environmental Effects on Composite Materials,* G.S. Springer, ed., Technomic Publishing Company Inc., Lancaster, Pa., 1981.

27. Davis, H.E., Troxell, C.E., and Wiskocil, C.T. *The Testing and Inspection of Engineering Materials.* McGraw-Hill, New York, 1955.

28. Springer G.S., ed. *Environmental Effects on Composite Materials, Vol. 2.* Technomic Publishing Company Inc., Lancaster, Pa., 1984.

29. Shen, C-H., and Springer, G.S. Moisture Absorption and Desorption of Composite Materials. In *Environmental Effects on Composite Materials*, G.S. Springer, ed., Technomic Publishing Company Inc., Lancaster, Pa., 1981.

30. Loos, A.C., and Springer, G.S. Moisture Absorption of Graphite-Epoxy Composite Immersed in Liquids and in Humid Air. In *Environmental Effects on Composite Materials,* G.S. Springer, ed., Technomic Publishing Company Inc., Lancaster, Pa., 1981.

31. Shen, C-H., and Springer, G.S. Effects of Moisture and Temperature on the Tensile Strength of Composite Materials. In *Environmental Effects on Composite Materials*, G.S. Springer, ed., Technomic Publishing Company Inc., Lancaster, Pa., 1981.

32. Shen, C-H., and Springer, G.S. Environmental Effects in the Elastic Moduli of Composite Materials. In *Environmental Effects on Composite Materials*, G.S. Springer, ed., Technomic Publishing Company Inc., Lancaster, Pa., 1981.

33. Adams, R.D., and Singh, M.M. Hydrothermal and Shear Loading of Polymer Composites. In *Progress in Durability Analysis of Composite Systems: Proceedings of the International Conference on DURACOSYS 95,* A.H. Cardon, H. Fakuda, and K. Reifsneider, eds. A.A. Balkema, Rotterdam, The Netherlands, 1996.

34. Smith, B.W. Fractography for Continuous Fiber Composites. *Composites, Engineered Materials handbook, Vol. 1.* ASM International, Metals Park, Ohio, 1987, p. 787.

35. Sloan, F.E, and Talbot, J.B. Evolution of Perhydroxyl Ions on Graphite/Epoxy Cathodes. *Journal of Electrochemical Society,* Vol. 133, No. 12, 1997.

36. Taylor, S.R., Stewart, K.C., and Cahen, G.L. *The Detection and Analysis of Electrochemical Degradation in High Temperature Polymer Matrix Composites.* Contract No. N62269-92-M-3271. University of Virginia, School of Engineering & Applied Science, Charlottesville, 1993.

37. Lin, T.L., and Jang, B.Z. *Polymer Composites.* Society of Automotive Engineers, Warrendale, Pa., 1990.